ASTRID2 – the UV and soft x-ray synchrotron light source with the ultimate brilliance

Niels Hertel, Søren Pape Møller and Jørgen S. Nielsen / 28-07-2009

1 INTRODUCTION AND GENERAL REMARKS

There has been a tremendous development of synchrotron radiation sources over the last two decades and this development has resulted in a subsequent expansion in the utilization of synchrotron radiation. The biggest quantum leap possibly came with the introduction of undulators, whereby the photon rate on a target increased by many orders of magnitude. To make full benefit of the undulators, small emittance lattices were developed. The ultimate limit of this increase in the brightness from synchrotron radiation storage rings is given by the "size" of the photons themselves, i.e. the so-called diffraction limit of $\lambda/4\pi$, where λ is the wavelength. Further increases in photon brilliance can only be obtained by coherent sources, such as free-electron lasers. Today, storage ring technology has reached the diffraction limit in the vertical plane even for X-rays, whereas in the horizontal plane the diffraction limit is still only accessible for soft X-rays.

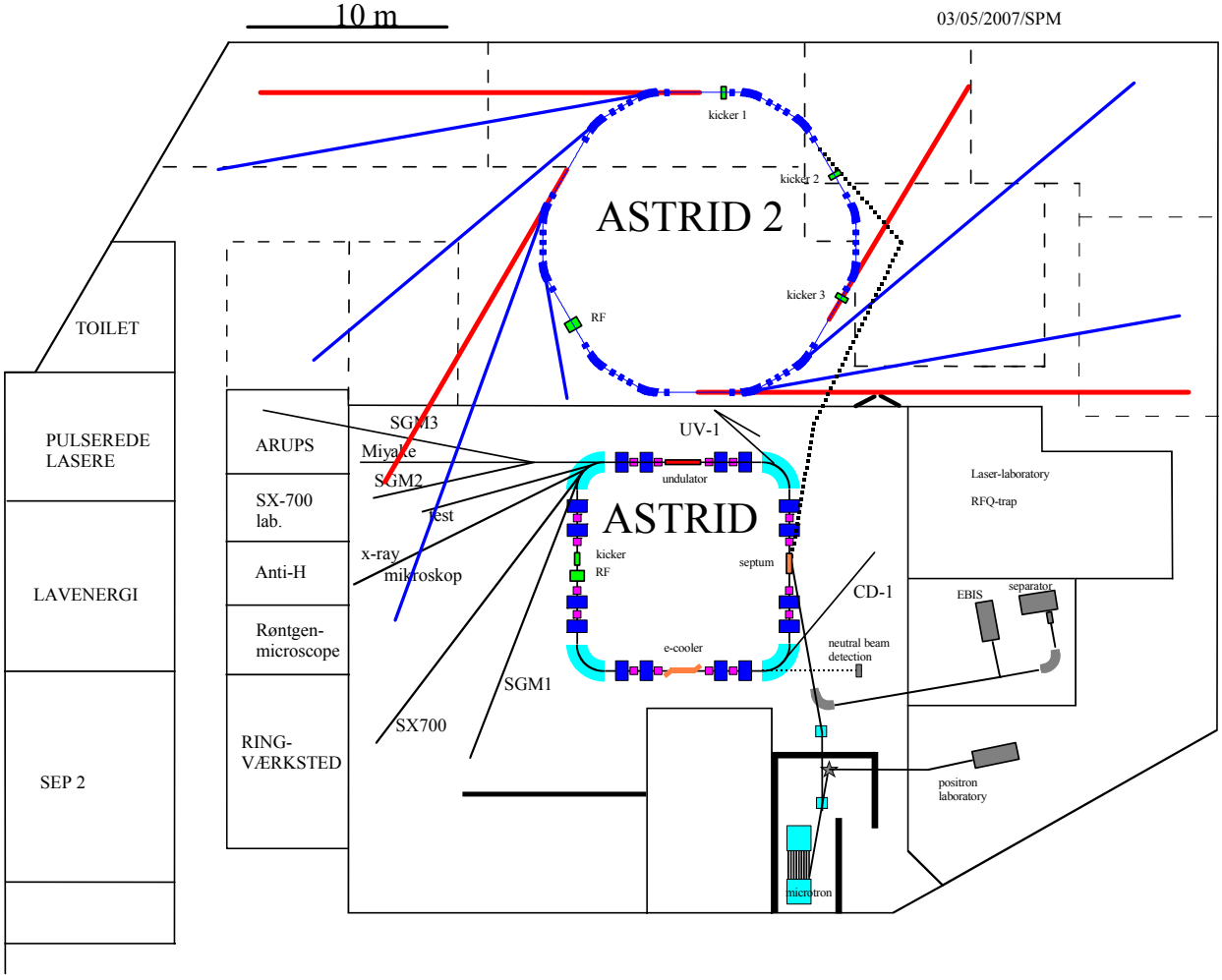

Fig. 1 Early drawing, prepared for the application, of the new synchrotron-radiation ring ASTRID2 in building with schematic representation of undulators and beamlines.

In the following, we will present the detailed design of the ASTRID2 storage ring. The radiation from this storage ring will be diffraction limited in the vertical plane for photons of almost all available energies and up to several tens of eV in the horizontal plane. For this reason we may call ASTRID2 a UV and soft X-ray source with the *ultimate brilliance*.

The document will present the design at the time of starting to order major components. Hence the document is also prepared in order to review the design.

As compared to ASTRID, the new machine will within the available physical space provide:
1: a state-of-the-art emittance much smaller than that of ASTRID
2: 4 straight sections available for insertion devices
4: much higher beam stability than at ASTRID
5: much better orbit control and feedback
6: easy injection and good lifetime
7: top-up injection from ASTRID

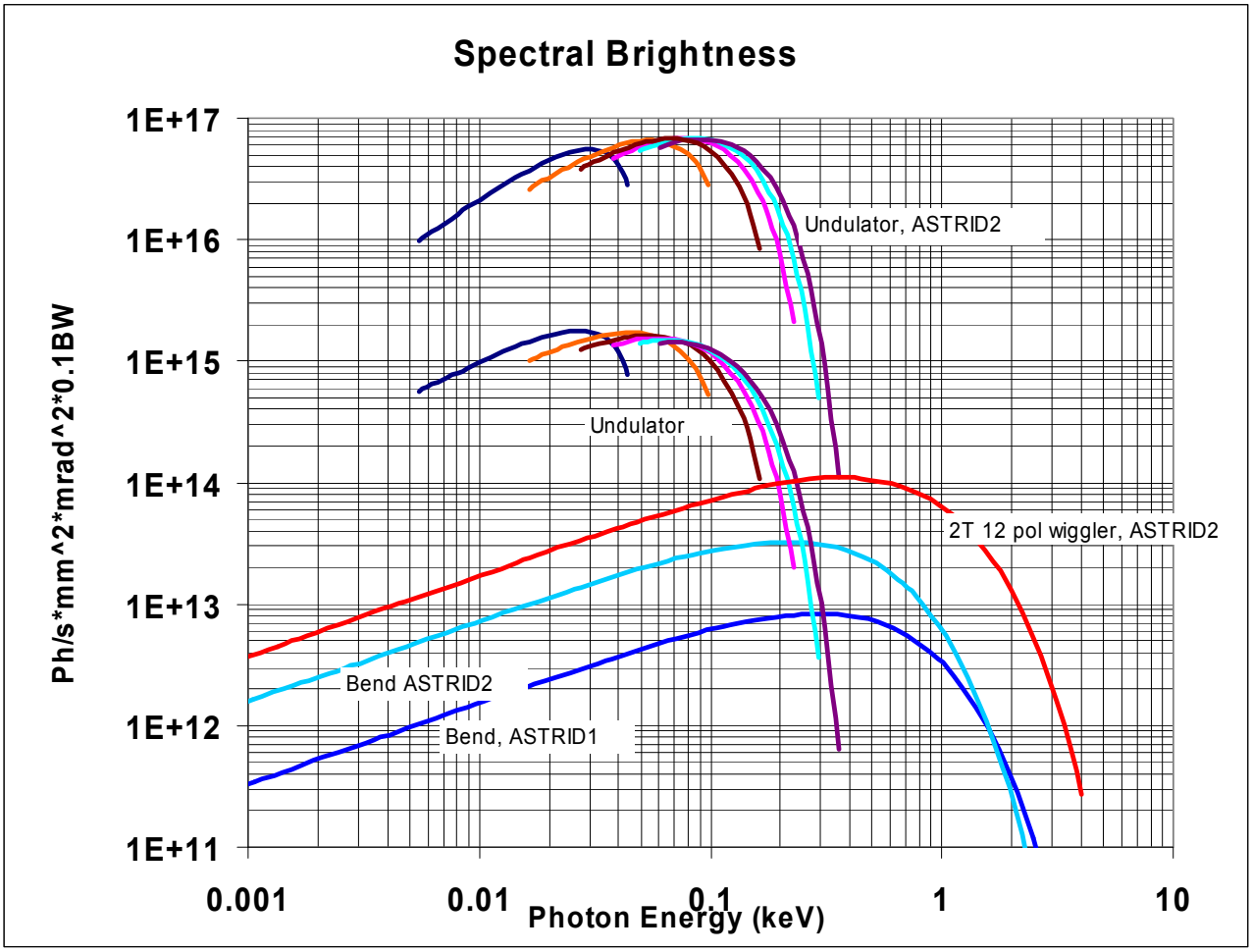

Fig. 2 Brilliance of the synchrotron radiation from the bending magnet for ASTRID and ASTRID2 and from the ASTRID undulator.

In the design of the ASTRID2 facility, we have chosen, as for ASTRID, to exclude X-rays in the regime above around 1 keV. Instead, we have chosen to concentrate on the UV, VUV and soft X-ray region, where we have expertise and have excelled, and where few facilities operate. Finally, although UV and soft X-rays are also obtained from high-energy storage rings, the use of low-energy radiation from a high-energy ring is severely compromised due to among other things the high heat-loads, the background radiation from higher energy photons, the potential damage on optics from the high flux of X-rays

and due to the large distances from the source making monochromators more complicated and expensive.

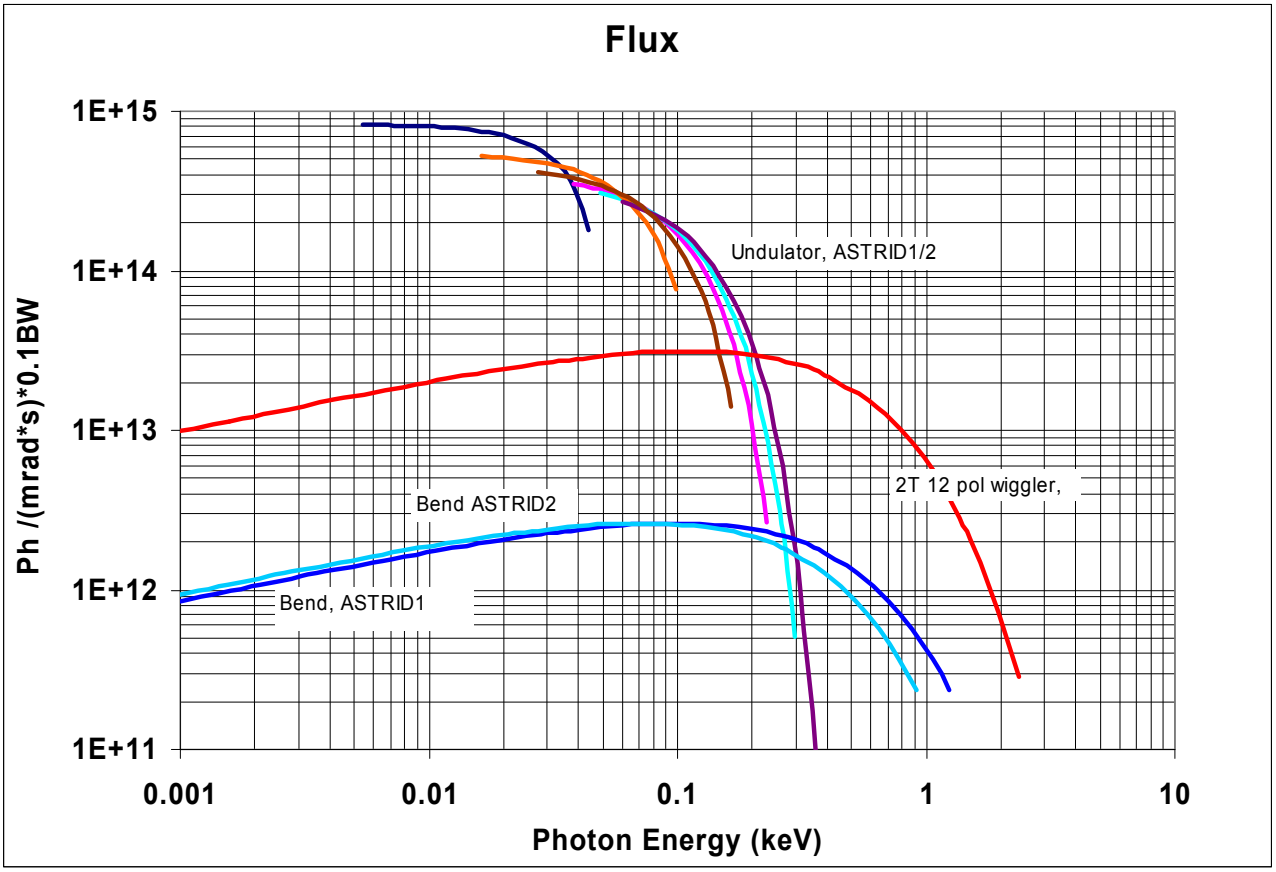

Fig. 3 Flux of the synchrotron radiation from the bending magnet for ASTRID and ASTRID2 and from the ASTRID undulator.

From these requirements and boundary conditions we have arrived at a hexagonal ring with an emittance of around 10 nm, see fig. 1. The electron energy will be 580 MeV, the circumference will be 45.71 m and there will be 4 straight sections available for insertion devices. It is planned to use ASTRID with its 100-MeV microtron as injector. This will ensure a short filling time to a large current, and allow top-up operation with very stable beam parameters. Small emittance storage rings will have modest lifetimes dominated by the Touschek lifetime, and for ASTRID2 the lifetime is predicted to be in the few hours region depending on the vertical emittance (see section 2.9). Hence frequent filling is necessary, and we will operate ASTRID2 with top-up injection at 580 MeV from ASTRID. This will result in almost constant photon intensities from ASTRID2 without any interruptions. To give a feel for the requirements to top-up operation, for a current of 200 mA and a lifetime of 5 hours, the current can be held constant to within 1% by topping up the current with 2mA every few minutes.

The characteristics of the synchrotron radiation spectrum appear from fig. 2 and 3, where the brilliance and flux for the existing undulator in ASTRID is given for the old ASTRID ring and the new ASTRID2 ring. For comparison, the brilliance from the bending magnets is shown too. For the new source, we observe an increase in the brilliance from undulators

by more than two orders of magnitude at low energies and much more at higher energies. The intensity of synchrotron radiation from bending magnets is increased by more than an order of magnitude. Similar increases can be expected for the number of photons hitting a target in a typical beamline.

The spectra discussed above were calculated for the existing undulator in ASTRID, but clearly the additional insertion devices planned for ASTRID2 will have to be selected corresponding to the required use. Choice of parameters will influence mainly the period length of the undulators, the peak field, the gap size, length, polarization etc. Small emittance storage rings, like ASTRID2, allows in particular a decrease in the vertical size of the vacuum chambers leading to smaller undulator gap heights. Increased intensities may be obtained at the highest energies up to around 1 keV from multi-pole-wigglers. In section 2.10, the chosen insertion devises will be described.

2 ASTRID2 – THE NEW LOW-EMITTANCE RING.

The boundary conditions for the design are many and include the available space, need for simplicity, small emittance (below the diffraction limit at low energies), injection from ASTRID at 580 MeV, an RF frequency identical to that of ASTRID of 105 MHz, and several straight sections. The proposed lattice of the storage ring has a 6-fold symmetry with a circumference of 45.714 m, corresponding to harmonic 16 of the RF frequency (ASTRID has h=14). The next larger size of the storage ring would correspond to harmonic 17 and a circumference of 48.571 m, uncomfortably large for the available hall.

2.1 Layout

The layout of the new ring appears from figure 4. It is displaced towards the south side of the hall with access around the ring along the outer wall towards the north and the chemistry department. The straight sections, starting with the injection straight, will have the following use:

SS1 at 2h: Injection septum magnet and kicker #2
SS2 at 12h: MPW for SX-700/SGM1 and kicker #3
SS3 at 10h: present ASTRID undulator
SS4 at 8h: RF and electron beam diagnostics section
SS5 at 6h: Future ID for ion-beam photon interaction experiment
SS6 at 4h: Future Insertion Device for short beamline

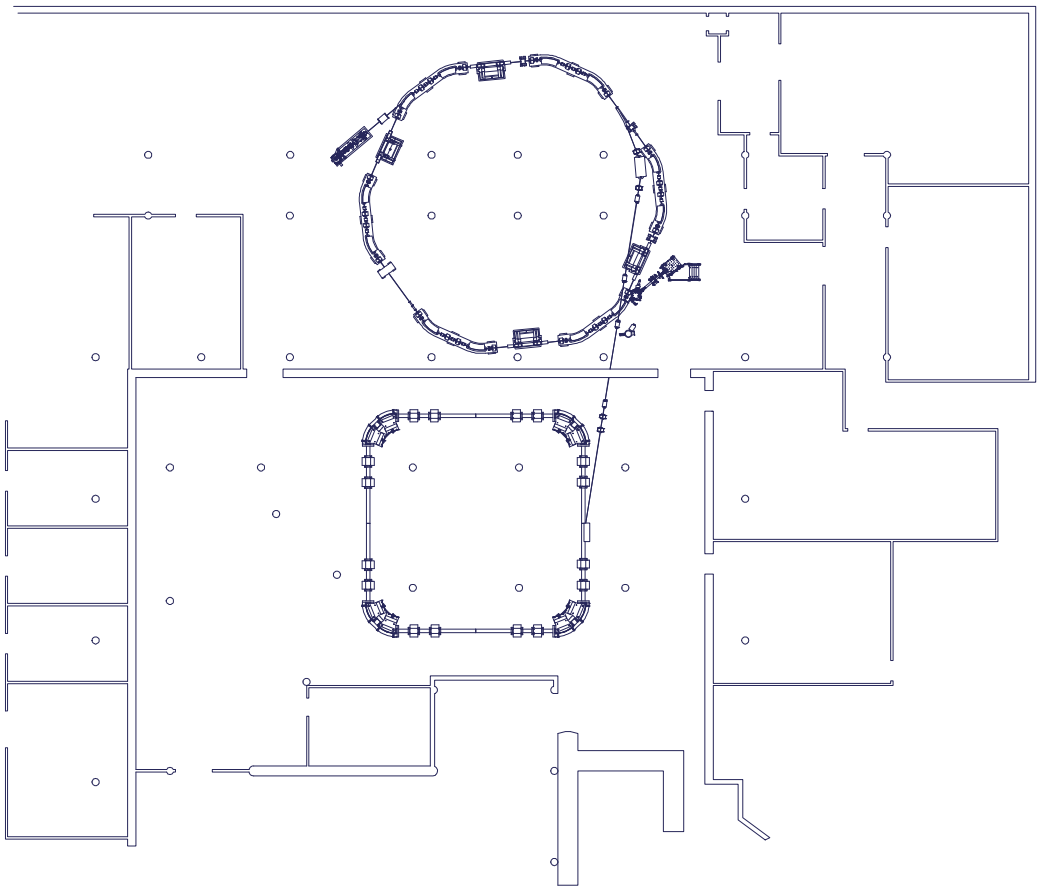

Fig. 4 Updated drawing of ASTRID2 placed in the available building.

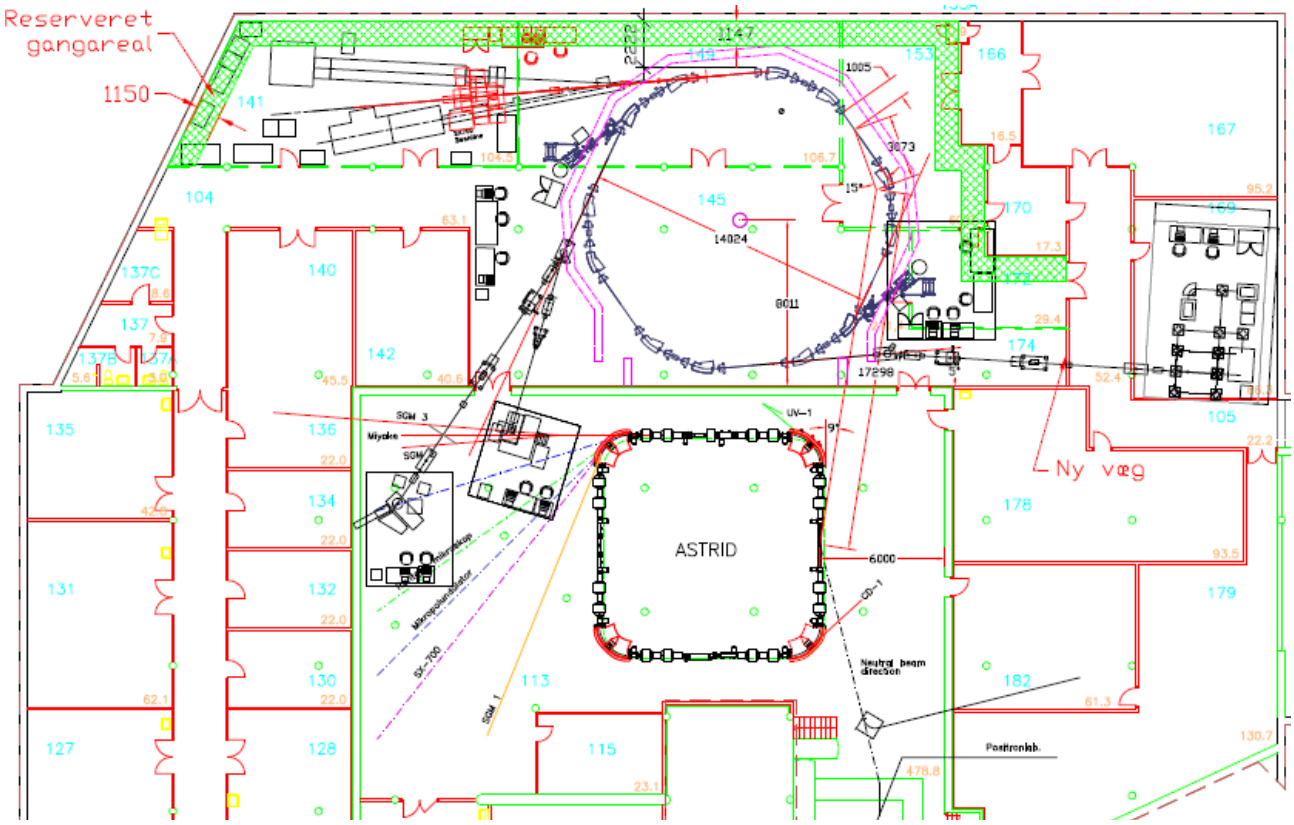

Fig. 5 Drawing of ASTRID and ASTRID2 with locations of beamlines and shielding wall around ASTRID2.

Four undulator beamlines with radiation from SS2, SS3, SS5 and SS6 will be possible, and in addition 6 bending magnet beamlines from 6 individual bending magnets. Injection is performed with a pulsed septum magnet in SS1 and three kicker magnets in SS1, SS2 and SS6. The RF system and other diagnostics equipment is placed in SS4.

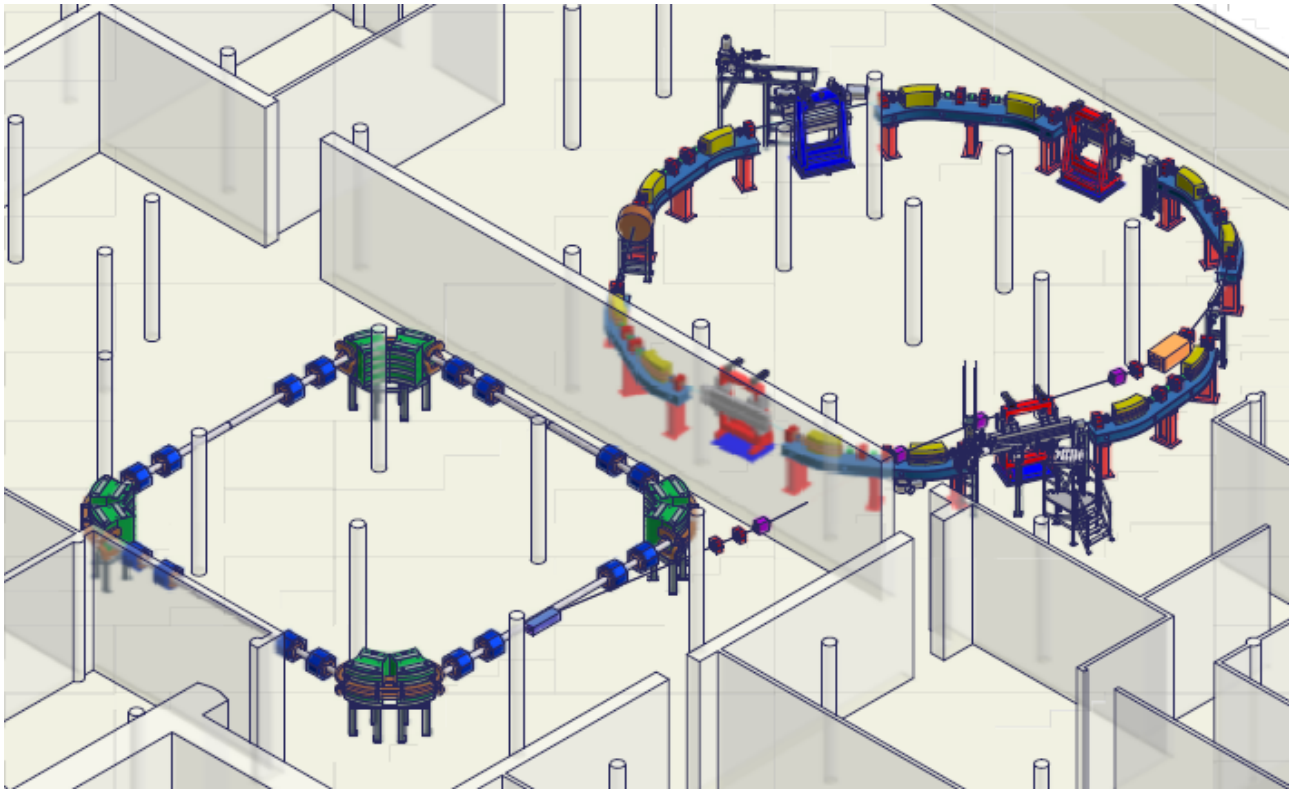

Fig. 6 Drawing of ASTRID, ASTRID2 and transfer beamline including pillars and walls. The location of the possible 4 insertion devices in ASTRID2 is also shown together with UV1 and CD1 beamlines.

2.2 The lattice

The lattice design (ast2_26.lat) of the ring is based on the use of combined function magnets (dipole and vertically focusing quadrupole fields in the main magnets), as this probably is the only way of achieving a very small emittance in small ring with a sufficiently large dynamical aperture. Some tune-flexibility is obtained using pole-face windings in the combined-function magnets together with the two horizontally focusing quadrupole families. However, the use of combined function magnets will limit the flexibility of the storage ring, although such flexibility is almost never exploited much anyway. A similar philosophy has been used at MAXLAB in their MAX 3 project. Similar combined-function magnets, as needed for ASTRID2, has been designed and built recently by DANFYSIK for the booster for the Australian Synchrotron Project, and this design has also be used for technical comparisons with the present project. In passing, we point out that ISA staffs have designed and commissioned this ASP booster.

Two families of sextupoles are inserted in the lattice, fig. 7: one family (of 6 sextupoles) in the middle of the arcs and one family next to the combined function magnets.

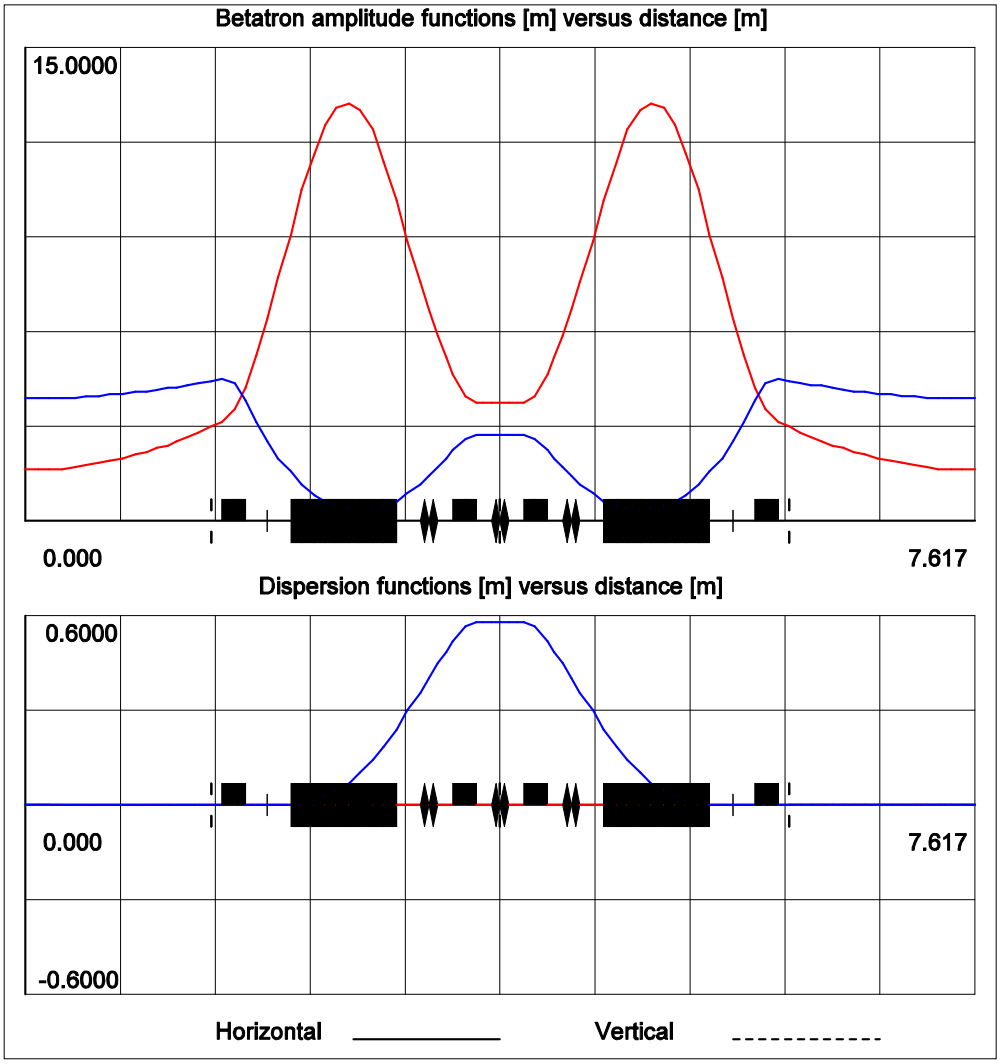

Fig. 7 Lattice functions for the zero-dispersion lattice over 1/6 of the circumference (ast2_26.lat).

We have chosen a variant of the lattice with zero dispersion in the straight sections, which leads to a natural horizontal emittance of 13 nm. A lattice with a finite dispersion in the straights can result in an emittance as low as half this emittance. However, we value a stable beam higher than a smaller beam. The optical betatron functions for the former lattice with vanishing dispersion in the straight sections are shown in figure 7. The corresponding horizontal and vertical rms beam sizes at 580 MeV are shown in fig. 8. The main parameters of the ring are given in table 1.

The above lattice is designed with sector magnets as this gives better defined magnetic fields, both dipolar, sextupolar and higher order multi-poles. The combined function magnets will be made from solid-cores and hence sector magnets are almost as easy to fabricate as rectangular magnets.

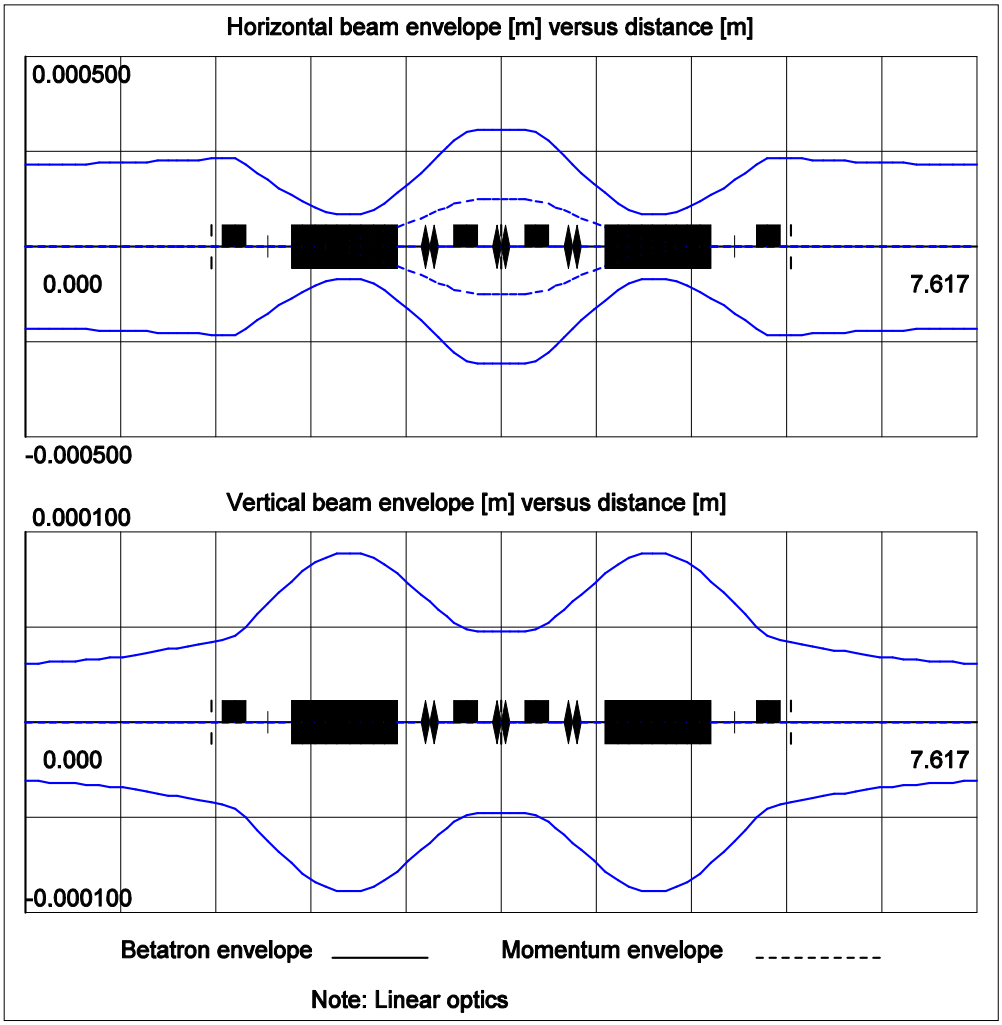

Fig. 8 RMS beam size over 1/6 of the circumference for the beam at 580 MeV with the nominal emittance of 12 nm horizontal and 0.6 nm vertical. Note the different vertical scales of 0.5 mm horizontally and 0.1 mm vertically.

Table 1 Main parameters of ASTRID2 storage ring (ast2_26.lat)

General parameters		**ASTRID2**	**ASTRID**
Energy	E [GeV]	0.58	0.58
Dipole field	B [T]	1.192	1.6
Circumference	L [m]	45.704	40.00
Current	I [mA]	200	200
Revolution time	T [ns]	152.45	133.43
Length straight sections	[m]	~3	
Number of insertion devices		4	1
Lattice parameters			
Straight section dispersion	[m]	0	2.7
Horizontal tune	Q_x	5.23	2.29
Vertical tune	Q_y	2.14	2.69
Horizontal chromaticity	$dQ_x/d(\Delta p/p)$	-6.4	-4.0
Vertical chromaticity	$dQ_y/d(\Delta p/p)$	-11.2	-7.1
Momentum compaction	α_p	0.0107	0.068
Coupling factor		5 %	5 %
Synchrotron Radiation parameters			
Synchrotron radiation integrals	I_1 [m]	0.488182	2.7164
	I_2 [m^{-1}]	3.870433	5.2016
	I_3 [m^{-2}]	2.384181	4.3060
	I_4 [m^{-2}]	-1.457685	1.8615
	I_5 [m^{-1}]	0.130774	0.9363
Energy loss per turn	U_0 [keV/turn]	6.2	8.3
Synchrotron radiation power	P_0 [kW]	1.2	1.6
Natural emittance	ε_H [nm]	12.1	140
Diffraction limit	λ [nm]	38-101	1759
Characteristic wavelength	λ_c [nm]	4.6	3.5
Characteristic energy	ε_c [eV]	267	358
Horizontal damping time	τ_h [ms]	20.7	29.1
Vertical damping time	τ_v [ms]	28.6	18.7
Longitudinal damping time	τ_s [ms]	17.6	7.9
RF parameters			
Damped energy spread	σ_E/E [0/00]	0.433	0.416
Damped bunch length	[cm]	2.2	6.5
RF frequency	[MHz]	104.950	104.950
Revolution frequency	[MHz]	6.56	7.5
Harmonic number	h	16	14
RF voltage	[kV]	50	30
Overvoltage factor	q	8.1	4
Quantum lifetime		∞	∞
Synchrotron frequency	$\upsilon=\Omega/2\pi$ [kHz]	10	20.6

2.3 Injection in ASTRID2

Injection, and accumulation, in ASTRID2 is made with a pulsed septum and three kicker magnets. The injection bump and the incoming beam are shown schematically in fig. 9. The shown bump corresponds to bumping the circulating beam 9 mm from the central orbit while injecting the beam at 16 mm. The 3-mm thick septum is located at 11.5-14.5 mm. Three kickers are needed to make the local bump as shown in fig. 9. Parameters of the extraction system are given in table 2.

Extraction of the beam in ASTRID will be performed with the existing dc septum magnet and a new fast kicker magnet, see section 3.1.1.

Table 2 **Injection in ASTRID2**

Injection energy	580 MeV
Horizontal emittance of beam from ASTRID	240 nm
Length of pulse from ASTRID	(133-50) = 83 ns
Horizontal/vertical rms beam size from ASTRID in SS center	2.00/0.16 mm
Horizontal/vertical rms beam size in ASTRID2 in SS center	0.22/0.03 mm
Injection Septum angle	15º + ? mrad
Thickness of septum (coil+vacuum chamber envelope)	3 mm
Aperture in septum channel	12×12 mm
Distance of inner septum envelope from center of ASTRID2	11.5 mm
Distance of beam from axis at exit of septum	11.5+3+1.5 mm
Length of septum magnet	1000 mm
Distance from center of ASTRID2 SS to beginning of septum magnet	834 mm
Septum pulse time	~100 μs
Distance from SS6 center to center of **Injection-bumper** magnet 1	+1234 mm
Distance from SS1 center to center of **Injection-bumper** magnet 2	-477 mm
Distance from SS2 center to center of **Injection-bumper** magnet 3	-1234 mm
Aperture in bumpers	40×28 mm
Nominal bumper angles for injection bumper 1, 2, and 3	-2.2,2.0,-2.5 mrad
Circulating beam trajectory bump at septum	9 mm
Bumper pulse time (½ sine wave)	1.6 μs

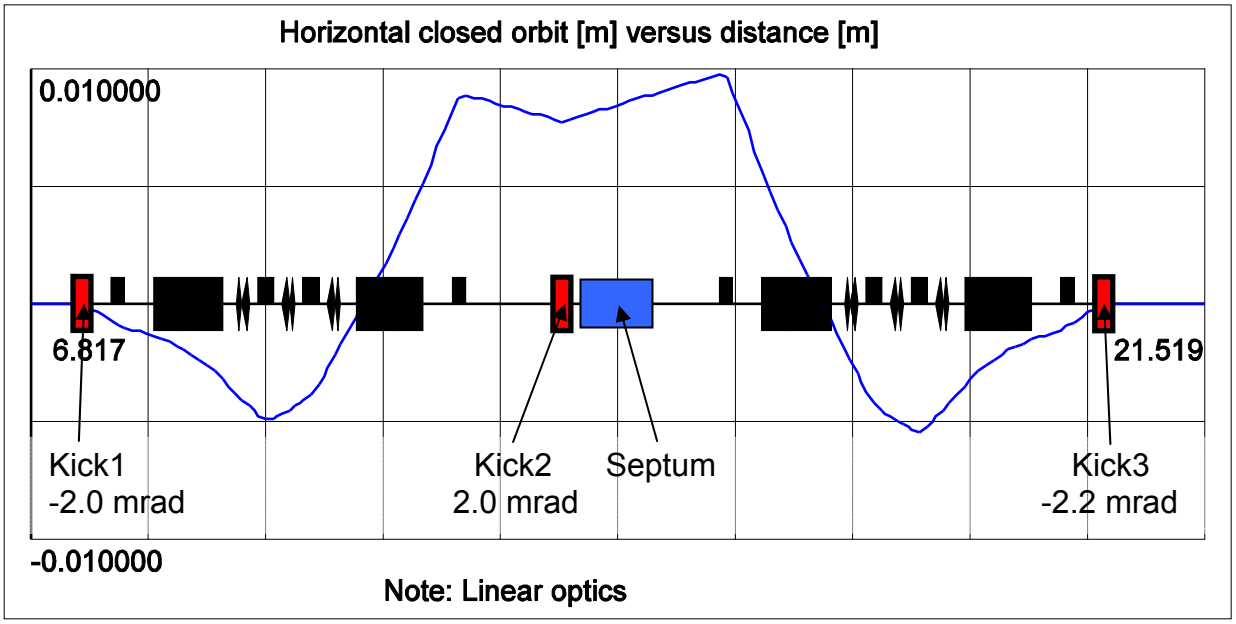

Fig. 9 Injection bump produced by the 3 kicker magnets. The three bump angles are indicated for the 9 mm bump at the septum.

2.3.1 Tracking simulations of injection process in ASTRID2

A tracking study of the injection has been made for the nominal optics of ASTRID and ASTRID2 corresponding to the numbers given in table 2.

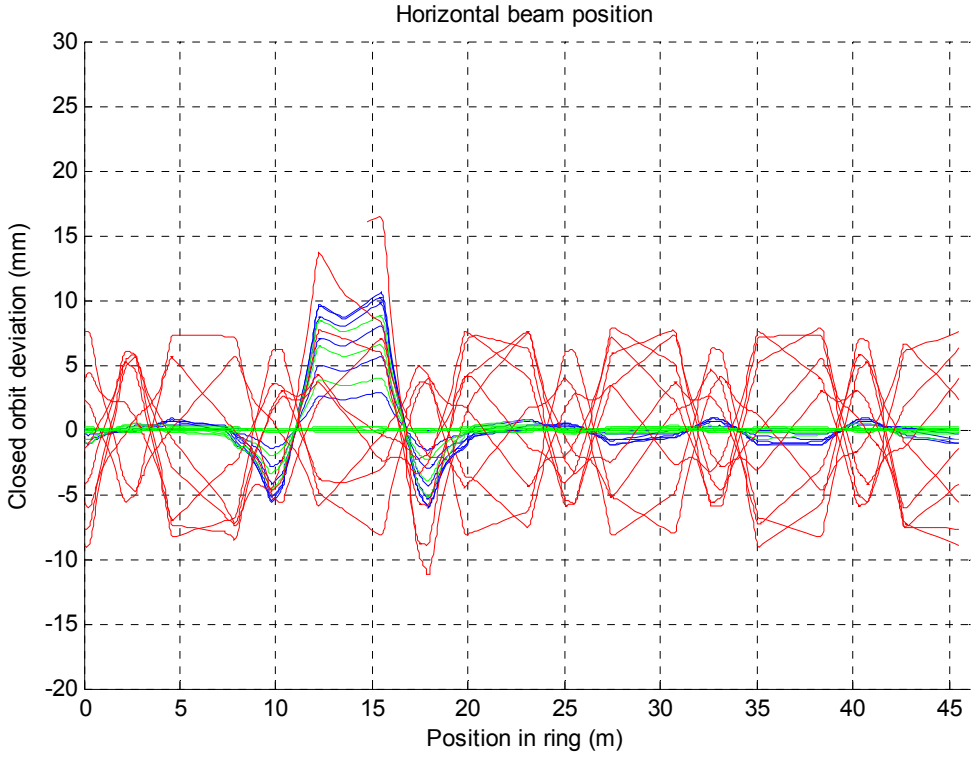

Fig. 10 Horizontal position during the first 15 turns. Red curves represent the injected beam, whereas blue and green correspond to the stored beam before and after injection.

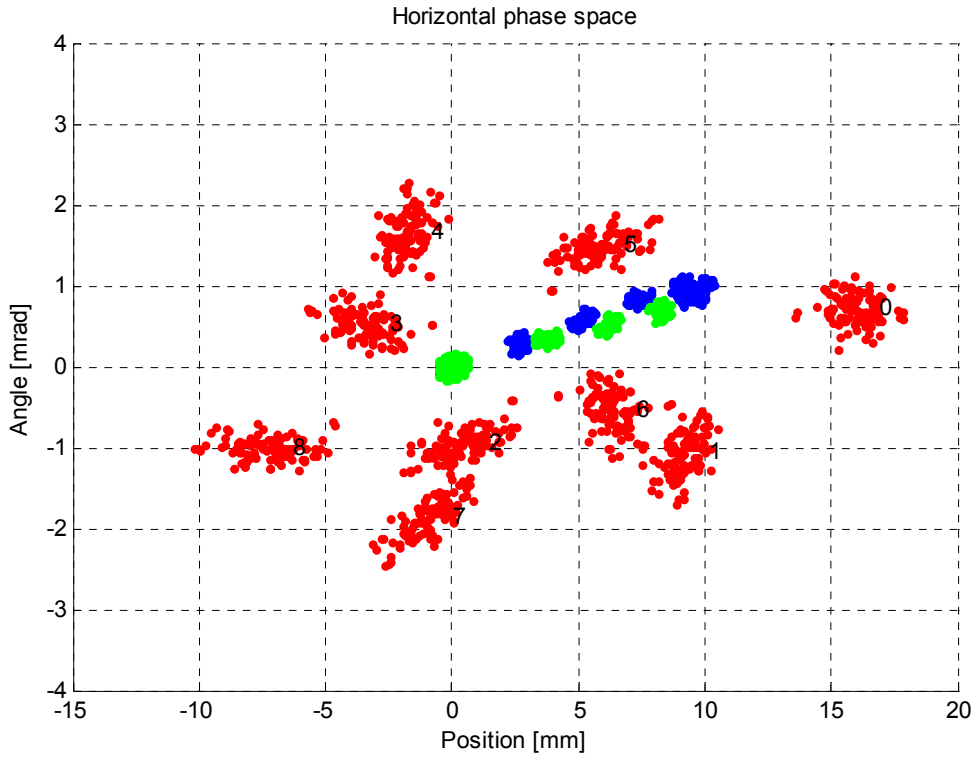

Fig. 11 The first 15 turns in transverse phase space. Red points are injected particles, whereas blue and green are stored electrons before and after injection.

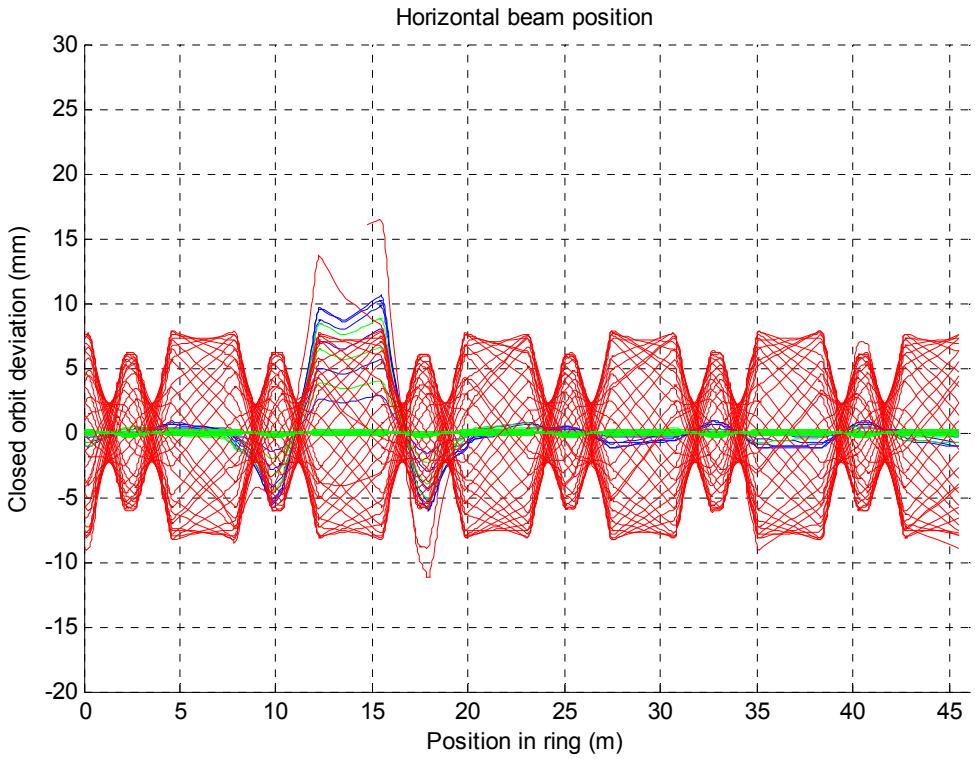

Fig. 12 Horizontal position during the first 40 turns. Red curves represent the injected beam, whereas blue and green correspond to the stored beam before and after injection.

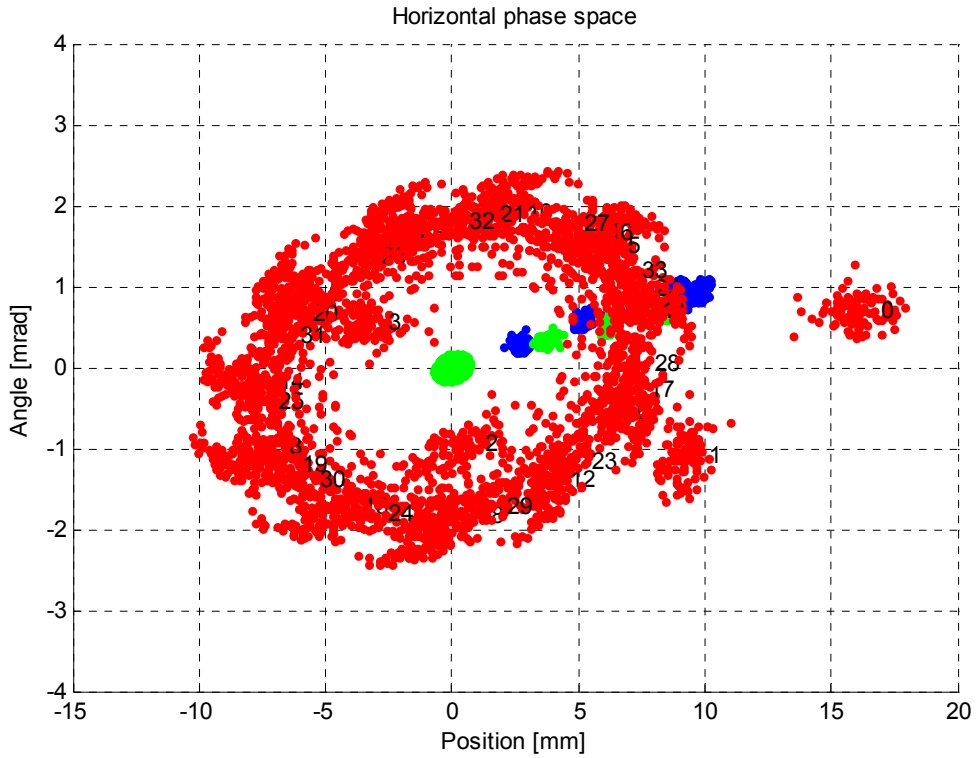

Fig. 13 The first 40 turns in transverse phase space. Red points are injected particles, whereas blue and green are stored electrons before and after injection.

2.4 Magnetic elements

The main parameters of the magnetic elements for ASTRID2 are given in table 3, 4 and 5. The 12 main deflection magnets are combined function magnets with included dipole and quadrupole fields. The two quadrupole families allow some tuning capabilities of the betatron tunes, in particular the horizontal tune but also the dispersion. In addition, pole-face windings will be installed in the combined-function magnets to tune the vertical tune ±0.1. Two sextupoles families will provide tuning of the chromaticities.

Table 3 Magnets for ASTRID2

Name of magnet	BD	Qf3/Qf2	Sd/Sf	
Type of magnet	Defocusing combined-function magnet	Quadrupole	Sextupole	HxV steerer
Number of magnets	12	12+12	12+6=18	12
Magnet length [m]	0.85	0.18	0.15	0.1
Aperture [mm]	44x28	Ø44	Ø44	45x45
Good field region [mm]	36x22	Ø36	Ø36	35x35
Dipole field [T]	1.1917	-	-	0.06
Radius of curvature [m]	1.6234	-	-	-
Quadrupole field [T/m)	3.2155	15 nom. 12.11/11.36	-	-
Sextupole field [T/m^2]	0	0	300 Nom. 143/220	-
Good field definition	$\Delta(\int Bdl)/\int Bdl$ $\Delta(\int(\mathrm{d}B/\mathrm{d}x)dl)/\int(\mathrm{d}B/\mathrm{d}x)dl$ $\Delta(\int(\mathrm{d}^2B/\mathrm{d}x^2)dl)/\int(\mathrm{d}^2B/\mathrm{d}x^2)dl$	$\Delta(\int(\mathrm{d}B/\mathrm{d}x)dl)/\int(\mathrm{d}B/\mathrm{d}x)dl$	$\Delta(\int(\mathrm{d}^2B/\mathrm{d}x^2)dl)/\int(\mathrm{d}^2B/\mathrm{d}x^2)dl$	$\Delta(\int Bdl)/\int Bdl$
Field accuracy	$5\cdot10^{-4}$ $1\cdot10^{-3}$	$1\cdot10^{-3}$	$4\cdot10^{-3}$	$1\cdot10^{-2}$
MPS	1 unipolar 10 ppm DC/slow ramp	1 unipolar 25 ppm DC/slow ramp	1 unipolar 100 ppm DC/slow ramp	2x12 bipolar 100 ppm DC/slow ramp

Table 4 Special magnets for ASTRID2 (numbers in parentheses refer to ASP booster)

Type of magnet	Fast extr. kicker magnet for ASTRID	Fast inj. Bumper magnet	Inj. septum magnet in ASTRID2
Number of magnets	1	3	1
Magnet length [m]	0.5	0.20	1.0
Aperture [mm]	80x24	44x28	12x12 in channel 40 x24 for stored beam
Good field region [mm]	72x22	36x22	36x22
Deflection angle	1.7 mrad (+30%)	3.5 mrad (2.2 nominal)	15°
Dipole field [T]	0.010	0.035	0.5 (+ 20%)
Radius of curvature [m]	200	57	3.869
Good field definition	$\Delta(\int Bdl)/\int Bdl$	$\Delta(\int Bdl)/\int Bdl$	$\Delta(\int Bdl)/\int Bdl$
Field accuracy	$1\cdot10^{-2}$	$1\cdot10^{-2}$	$1\cdot10^{-3}$
Max. leak field on central orbit	$\int Bdl$		0.1 gauss m
Number of MPS	1 unipolar fast risetime <50ns	3 unipolar sine wave (~1.6μs)	1 unipolar sine-wave (~100μs)

Table 5 Magnets for transfer beamline ASTRID → ASTRID2 (Q-poles and steerers are identical to those in ASTRID2)

Type of magnet	Beamline Dipole (V)	Beamline Dipole (H)	Beamline quadrupole	HxV steerer
Number of magnets	4	1	4	4
Magnet length [m]	0.3	1.0	0.18	0.2
Aperture [mm]	30x45	45x30	Ø44	45x45
Good field region [mm]	18x24	24x18	Ø36	24x18 (id)
Deflection angle	4.3°	30°		6 mrad
Dipole field [T]	0.48	1.013		
Quadrupole field [T/m)			15 (nom. <5.6)	
Good field definition	$\Delta(\int Bdl)/\int Bdl$	$\Delta(\int Bdl)/\int Bdl$	$\Delta(\int(\mathrm{d}B/\mathrm{d}x)dl)/\int(\mathrm{d}B/\mathrm{d}x)dl$	$\Delta(\int Bdl)/\int Bdl$
Field accuracy	$5\cdot10^{-3}$	$5\cdot10^{-3}$	$1\cdot10^{-2}$	$1\cdot10^{-2}$
Radius of curvature [m]	2.86	1.69		
Number of MPS	1 unipolar 25 ppm DC	1 unipolar 25 ppm DC	7 unipolar 25 ppm DC	2x4 bipolar 100 ppm DC

2.5 Closed orbit errors and correction

Closed orbit correction will be made with a system of 18 (POSSIBLY only 12) beam-position monitors and 12 combined horizontal and vertical correction dipole magnets. For the operating tunes of 5.23 and 2.14, these numbers are maybe a little on the low side in the horizontal plane and quite reasonable in the vertical plane. The BPM's will be placed in the beginning and at the end of the straight sections close to the quadrupoles and possibly in the middle of the arcs, whereas the correctors will be placed between the quadrupole in the straight sections and the dipoles. Additional correctors in the middle of the arcs do not improve the correction capability.

Closed orbit errors have been simulated using the nominal lattice using WinAgile. We have assumed the following magnetic and alignment errors:

Table 6 Magnet and alignment errors for ASTRID2

Horizontal kick error	0.26 mrad ~$\Delta B/B=5\cdot10^{-4}$
Vertical kick error	0.05 mrad ~$\Delta B/B=1\cdot10^{-4}$
Axial shift of dipoles	0.15 mm
Transverse shift of quadrupoles	0.10 mm

The errors given in table 6 are rms errors cut at 2 rms. The errors predicted from the simulation appear from fig. 14.

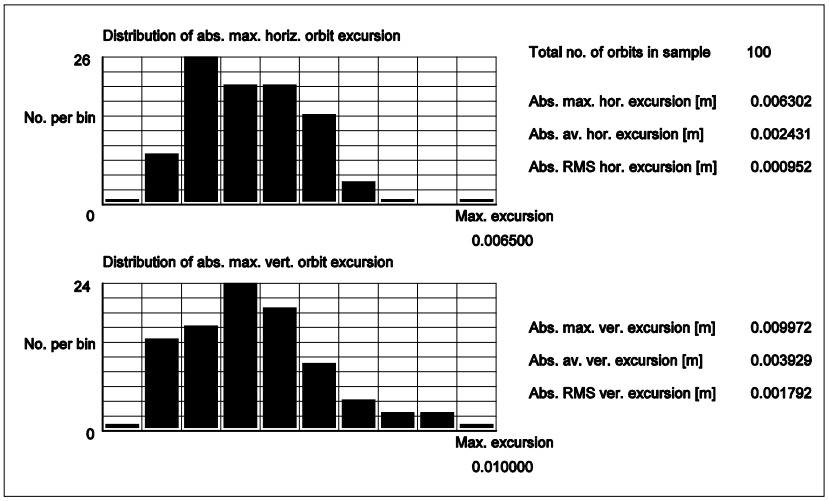

Fig. 14 Maximum horizontal and vertical orbit excursions.

Maximum excursions of up to 6 and 10 mm are observed in the horizontal and vertical planes, respectively, with average vertical excursions of 2 and 4 mm. These should be small enough to secure a stored beam without closed-orbit corrections.

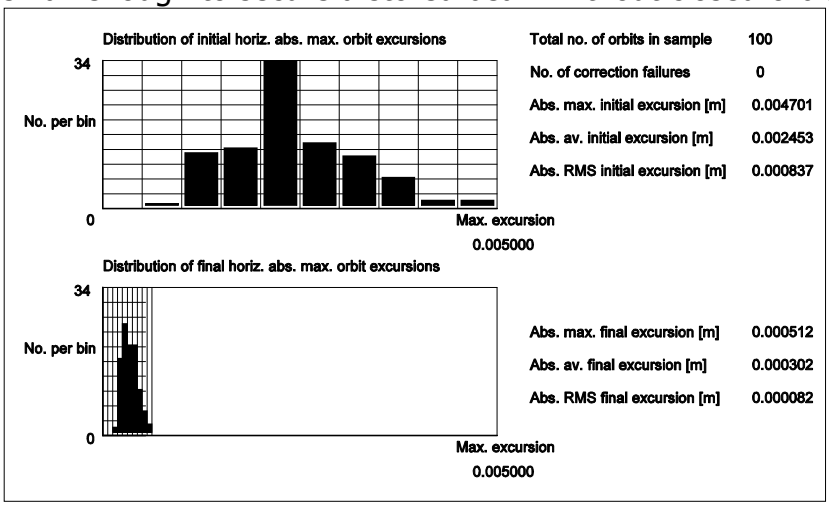

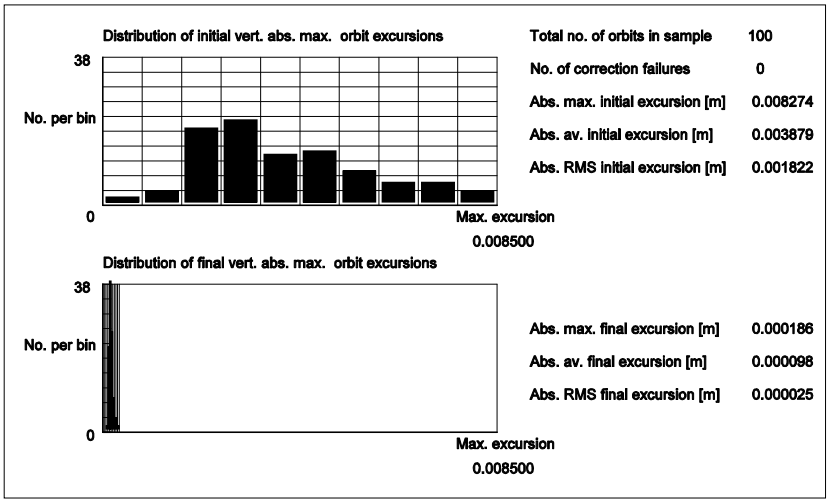

Fig. 15 Un-corrected and corrected closed-orbit errors.

The orbits can be corrected to maximum excursions of 0.5 and 0.2 mm, fig. 15, in the horizontal and vertical planes, respectively. This is all made for 18 BPM's as described above. Use of only 12 BPM's in the straight sections gives rise to 1.0 mm maximum excursions horizontally and still 0.2 mm vertically.

Simulations have also been made using MATLAB and the Accelerator Toolbox. We have used rms transverse shifts of the quadrupoles of 0.1 mm and main dipoles, rms rotation angles of the quadrupoles of 1 mrad for quadrupoles and 0.1 mrad for dipoles. Maximum excursions of up to 4.3 and 13.1 mm in the horizontal and vertical planes are observed. The corresponding average maximum excursions are 1.9 and 6.2 mm. The results are slightly higher than the above results obtained with WinAgile, but with MATLAB the random errors are not cut at 2 RMS. Furthermore, also combined-function dipole displacements are included. Actually, the vertical displacements of these dipoles of 0.1 mm rms are the largest contributor to the closed orbit deviations.

In addition to a good closed-orbit control as described above, which will secure a good injection efficiency and lifetime, local control of the orbit in the straight sections with its insertion devices is also mandatory for adjustments of the synchrotron radiation down the beamlines, and for possible compensation of undulator errors. One way of varying the position and angle of the closed orbit in the straight sections, in addition to global closed-orbit correction, is to use local position and angular bumps. In fig. 16 simulated horizontal and vertical local position and angular bumps using 4-magnet bumps are shown.

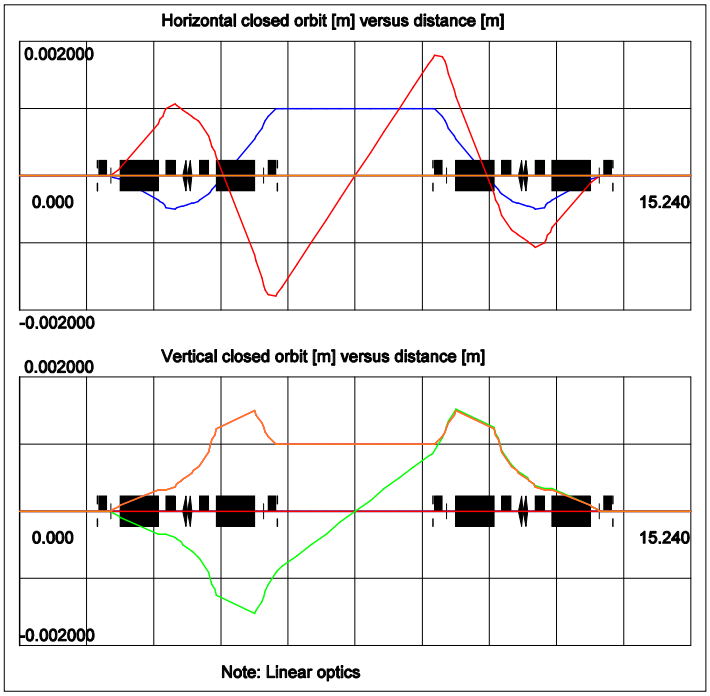

Fig. 16 Local horizontal and vertical local 4-corrector position and angular bumps.

2.6 RF system

The RF system will in many ways will be similar to the present ASTRID system. The frequency of the system will nominally be 104.950 MHz, similar to the ASTRID nominal

frequency. We plan to have a setup where ASTRID and ASTRID2 can operate using the same master oscillator, which will allow easy synchronization (phase matching) of the two rings. For debugging of ASTRID we will also have the possibility to operate ASTRID with a separate master generator.

A new semi-digital semi-analog LLRF will be built. This system will first be built for ASTRID and tested there as the ASTRID system needs to be replaced. It is planned to build a capacitatively loaded cavity like the ASTRID cavity and what recently has been built at MAXlab for MAX 2 and 3. The cavity will be made from solid copper. Tuning will be made by squeezing the cavity. As several new cavities are needed for MAX 4, we are aiming to use their fabrication technology and as far as possible exploit their experience and collaborate.

2.6.1 Main cavity

The main RF cavity will be a stub type capacitively-loaded cavity, similar to our present ASTRID cavity. A suitable new cavity, which will fit our needs very well, is the "Lund-cavity" developed for MAX 2 and 3 ("The 100 MHz RF System for MAX-II and MAX-III", Å. Andersson *et al.*, Proc. of EPAC 2002, 2118). This cavity was developed for 100 MHz, and will not need much modification for operation at 105 MHz. The "Lund-cavity" is designed for 30 kW, which is significantly more power than we will need (see next subsection). The shunt impedance of the "Lund" cavity is 1.6 MΩ, whereas it is 1.4 MΩ for the ASTRID cavity.

In order to allow for future upgrades we will reserve space for a possible future Landau cavity in ASTRID2.

2.6.2 Transmitter

It is planed to acquire a tube-based class AB FM transmitter for ASTRID2. At ASTRID, a tetrode based 20 kW FM transmitter has worked very well for many years. This transmitter has been retuned slightly, so that it now is somewhat more broadband. This has reduced the maximum output power to ~8 kW. The reason for the need of the wider amplification range is the Fast Feedback Loop, which was developed to make injection easier in ASTRID. At ASTRID the rf system has always been operating without a circulator, and this is also the plan for ASTRID2. Table 7 shows the power needed for ASTRID2 and for comparison also for ASTRID. A wide range in cavity voltage is specified as it is still uncertain which cavity voltage is optimal from a lifetime perspective (higher RF capture range gives a higher lifetime), see sec 2.9 for lifetime considerations.

Table 7 RF power requirements for ASTRID2 and ASTRID (for I=200mA)

	ASTRID2	**ASTRID**
Cavity Voltage, V_{cav}	50-100 kV	38 kV
Cavity Shunt Impedance, R_s	1.6 MΩ	1.37 MΩ
Cavity power ($V_{cav}^2/(2R_s)$	0.8-3.1 kW	500 W
Bending magnets SR power	1.2 kW	1.6 kW
"ASTRID" undulator	18 W	18 W
New ASTRID2 undulator	54 W	

MPW	328 W	
Future new ASTRID2 undulator	100 W	
Total power need	2.5-4.8 kW	2.1 kW

2.6.3 Low-Level RF (LLRF)

For the LLRF for ASTRID2 we have several options: 1. a copy of the old ASTRID analog LLRF (this is not likely to be a good solution), 2. a fully digital solution based on digital down and up conversions, and a FPGA-like processor for calculation, or 3. a kind of combination, where we have the control of the regulation loops in software, but use analog components to control the actual RF signals. The last option is the most likely implementation. Here we envisage use of phase comparators and amplitude detectors to get information on the RF signals. The output voltages from these detectors (with bandwidths up to (many) kHz) are feed into a fast real-time computer. The real-time computer then performs the necessary calculations find to the optimal values of the RF signal driving the cavity. We envisage to use voltage controlled attenuators and phase shifters for the actual control of the RF signals. As an alternative to work with phase and amplitude we could also work with *I* and *Q*, using *IQ* modulators and demodulations. Components for use around 100 MHz for both IQ and phase/amplitude setups are commercially available.

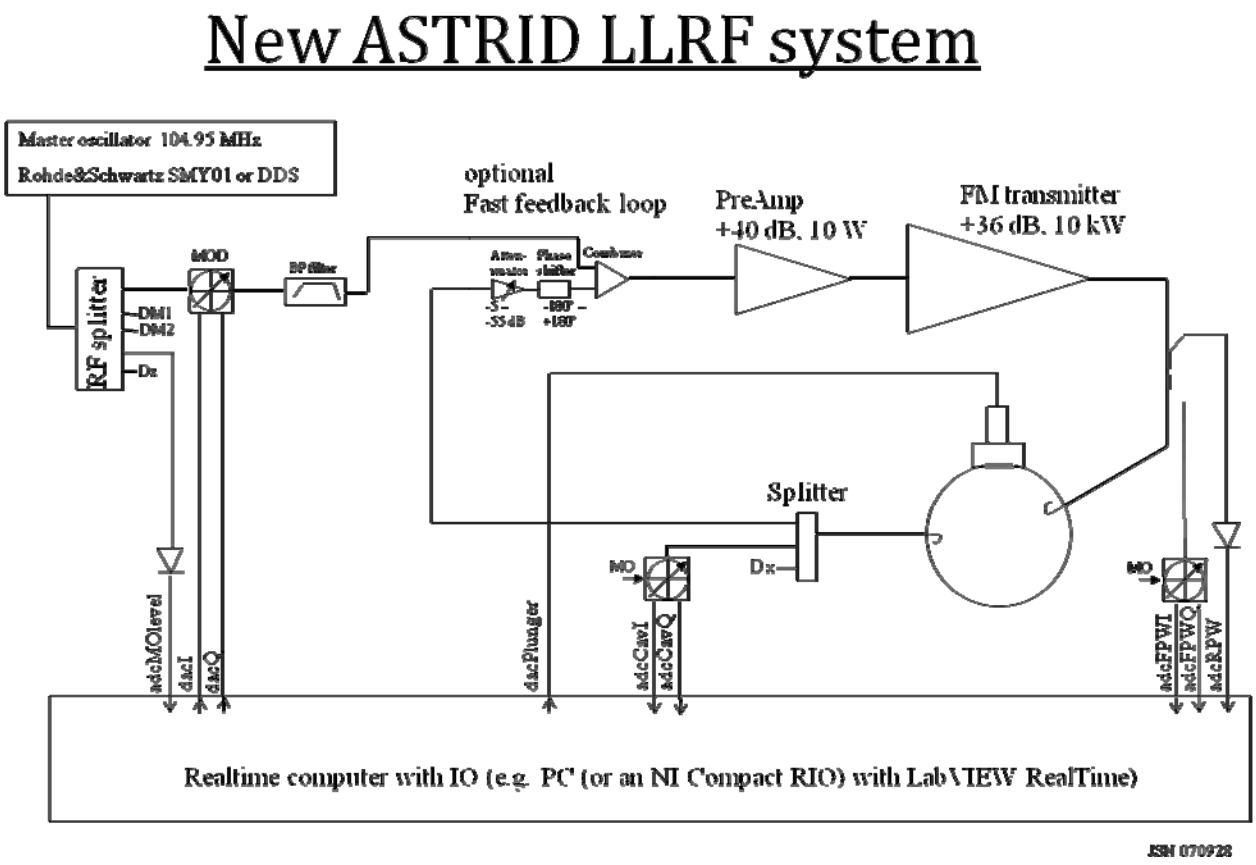

Fig. 17 Sketch of the new Astrid LLRF (IQ version).

The real-time computer could be a standard (server grade) PC running LabVIEW Real-Time. For input and output we envisage commercial PCI ADC/DAC data acquisition cards, for instance from National Instruments. With such a system we should easily obtain regulation-bandwidths of several kHz, which we believe should be more than sufficient. (With a Q of several thousands, the filling time of the cavity will be on the order of 10 µs, limiting the rate of external change of the cavity voltage to about ten kHz.). The regulation loop is foreseen to be a PID loop.

With a proper control program, we can also draw diagnostic signals out of the system. This could be for diagnostic of the regulation loops, both with the loop closed (error signals) and open (measure for instance the open loop responses). This will help achieving the best regulation loop settings. The diagnostic bandwidth does not need to be limited to the same bandwidth as for the regulation. On the contrary, we will seek to achieve as high a bandwidth for the diagnostic as possible within the frame of affordable data acquisition cards.

LabVIEW Real-Time allows the system to be controlled/viewed through a Web-interface, and it will of course also be easy to interface it to our control system, if not directly then certainly through the use of Shared Variables and a Gateway PC.

We do not plan to install a Fast Feedback Loop on ASTRID2, but since this is needed for ASTRID (in SR mode) there will be an option in the LLRF for it. As the LLRF for ASTRID is very old and not easy to maintain, we have decided to make the first system (a prototype) for ASTRID.

2.7 Beam diagnostics

A modern synchrotron light source is very dependent on having all the necessary beam diagnostics devices, both for the initial commissioning and later also for successful daily operation.

Table 8 gives an overview of the beam diagnostics elements which will be implemented for ASTRID2.

Table 8 ASTRID2 beam diagnostic

Type	**Purpose**
DCCT	Current measurement
FCT (Fast Current Transformer)	Injection (optimizations, loss, …)
Viewer, OTR or fluorescence One after septum (dual stroke), and one in RF straight	Commissioning (Injection detection) (injection) Emittance measurement (Check of transport line lattice, (Qpole scans))
EBPM (Electronic Beam Position Monitor, 12 (18?) BPMs)	Orbit monitoring and orbit correction
Slow orbit correction (1 Hz)	
Q-pole shunts (shunt resistors at 0.5%, **1%, 2%**, 4%)	BPM offset calibration Additional beam position monitors Lattice measurements (beta functions, LOCO)

SR cameras, two sets	Emittance measurement Visual check (instabilities, drifts, …) Injection optimization (feedback on SR light position (maybe also during top-up if possible)
Striplines, 45°, two sets (measure and excitation) Injection straight and RF straight	Tune measurement Commissioning (Injection detection)
Striplines, 90°, RF straight	Excitation (vertical betatron excitation for lifetime improvement) Excitation for feedbacks (TMBF)
2 BPM for diagnostic, RF straight and injection straight	Detector for feedback General pickup
A ring formed pickup (short tube), RF straight	Longitudinal pickup for (RF) diagnostic.

2.7.1 Current measurement and viewers

For determination of the stored current a DCCT will be used. We expect to use a commercial product like the Bergoz NPCT-CF4"½-60.4-120-UHV. The DCCT is planned to be installed in the RF/Diagnostic straight section (SS4).

Primarily to tune the injection process a Fast Current Transformer (FCT) will be installed (propably) just after the septum in SS1. This FCT is likely to be a Bergoz FCT-CF6”-60.4-40-UHV, which can be installed directly in the vacuum chamber. The FCT can also be used to monitor the bunch length of the stored beam.

Again to facilitate the injection commissioning two viewers will be installed. One dual-stroke just after the septum, can monitor and position the beam coming out of the septum, and again after one turn in the machine. Another (single-stroke) viewer will be placed in the RF/Diagnostic straight, able to monitor the beam after half a turn. Besides giving a visual view of the injected beam, the viewers can also be used to measure the beam size. Measuring the beam sizes for various settings of quadrupole magnet currents, will allow measurement of the optical parameters of the beam, and can provide a check of the optical elements. The viewers will most likely be based on Optical Transition Radiation (OTR) since these (as opposed to fluorescence screens) will have no problem with saturation of the emitted light, and no problem with degradation of the fluorescence material. There should easily be sufficient intensity of the emitted light, due to the high beam energy (580 MeV) and high electron beam intensity (several mA’s and a pulse width of ~50 ns).

2.7.2 Synchrotron radiation monitors

At two places around the circumference we plan to install cameras to monitor the synchrotron radiation light emitted from the electrons circulating in the machine. These detectors can be used to determine the emittance of the beam, and they will provide a non-destructive visual view of the beam, which can be essential to diagnose instabilities in

the beam. The positions of the SR monitors are expected to be at the first dipole magnet after the septum and at the first dipole magnet after the RF/diagnostic straight. These positions cannot easily be used for beam lines, because of physical space limitations.

2.7.3 BPM system and Orbit correction

ASTRID2 will be equipped with 12 sets of Button Pickups, located at the ends of the arcs as close as possible to the QF1 focusing quadrupole magnets. Having the BPM's at the ends of the arc, will give the best ability to position the beam in the straights, and hence have the best control of the angle and position of the light from the insertion devices.

It is at present undecided whether the BPM's will be one (commercial) block (with flanges) or whether the BPM's will be made as an integral part of the vacuum chamber. For the latter system we envisage four small 'hats' which will house the buttons, and allow the buttons to be level with the chamber. SMA connectors are planned as feedthrough's. Good quality cables will bring the signals to centrally placed electronics.

The electronics are expected to be an analog multiplexed system like the Bergoz MX-BPM system, which we have had quite good experience with for a small number of BPM's at ASTRID. On ASTRID, with quite large vacuum chambers (d=70-150mm) we routinely achieve precisions (noise) of ~1μm. With the smaller chamber dimension (d=38mm) for ASTRID2, we should easily achieve the same or better precision, which will be sufficient. The vertical beam size will be on the order of 50μm, and with the usual rule of thumb that it is necessary with a precision of 10%, we have plenty of margin.
To achieve the necessary accuracy (i.e. absolute with respect to nominal orbit) we plan to install Q-pole shunts at all of the quadrupole magnets. If the beam is not going in the center of a quadrupole magnet, the beam will move when shunting some of current in the quadrupole magnet. By monitoring the position change in the nearby BPM, the beam can be steered so it goes through the center of the quadrupole (i.e. so the beam does not move when shunting some of the current). The resulting position in the BPM can now be used as offset, giving absolute (with respect to the Q-poles) precision of the BPM's. By installing Q-pole shunts also at the QF2 quadrupole family (between the dipole magnets) we will have the possibility of centering the beam here too.

The orbit correction will only be a slow correction (~1 Hz), since the small dimension of the ring should make this sufficient. We have no plans for a fast orbit correction (>~10 Hz).

The Q-pole shunts are planned to be 2-4 power resistors, which via a relay can redirect some of the current. The individual resistors should redirect a few percent in binary steps, say 0.5%, 1%, and 2%. Besides the possibility of measuring the beam position in the quadrupole magnets, the Q-pole shunts will allow measurements of beta functions, and determination of more lattice functions for instance by the LOCO method.

It is been considered whether it would be better to have a more advanced button readout electronics, like the Libera system, but is has been decided not to use this sytem.

2.7.4 Pickup and exciters (striplines)

We plan to install three sets of striplines. Two sets at an angle of 45°, and one set at 90°. The two sets at 45° (one set placed in the injection straight and one set placed in the RF/diagnostic straight) will be used as very sensitive pickups (for commissioning of the machine), and for tune measurements. The 90° stripline will be used for excitations, for instance for transverse feedbacks, or possibly for vertical excitation for lifetime enhancements.

Tunes will be measured using a spectrum analyzer with a tracking generator. The beam will be excited using one 45° stripline, and the response (either another stripline in the same set or a stripline from the other set of striplines) will be measured by the analyzer.

Two extra sets of button pickups will be installed, one in the injection straight and one in the RF/diagnostic straight. These will be used as pickup detectors, for instance for future feedback systems. In the RF/diagnostic straight we will also install a short ring electrode to get a more sensitive signal for longitudinal diagnostic.

Initially, no feedback systems will be installed, but the ring will be prepared for easy installation of transverse feedbacks. For longitudinal feedback space will reserved in the RF/diagnostic straight to allow installation of a longitudinal kicker. Likewise a Landau cavity will not be installed initially, but we will reserve space for a Landau cavity at a later stage.

2.7.5 Instrumentation

Table 9 gives an overview of the instruments for ASTRID2. The philosophy chosen is that all instruments should be located at the machine, and accessed remotely (via LAN) from the control room. This makes cabling much easier and high signal qualities can be maintained. The cameras for viewers and SR light detection are also expected to be with LAN interface (GigE).

Table 9 ASTRID2 instruments

Type	**Purpose**	**Possible model**
Fast Scope (BW: ≥1GHz, Sample rate: ≥4GS/s, 4 ch.)	Monitor of fast signals (injection (strip lines, BPMs), monitor signals from fast elements (septum, bumpers, …), RF, triggers,)	Lecroy 104Xi-A or a Agilent 9000
Multiplexer for fast scope	To allow for remote selection of inputs for the fast scope	Agilent 34980A with 34941A multiplexers or Agilent 34970A with 34905A multiplexers
Spectrum Analyzer	Tune measurement, sensitive injection detection	Agilent N9320B

2.8 Vacuum and bake-out philosophy

The vacuum system is at present (july 2009) being designed and only some general comments will be made here.

One of the major decisions will be, whether we will build an in-situ bake-out system or an ex-situ system as built for e.g. the Australian Synchrotron Project. The advantages of either system are obvious, and will not be repeated here, but we will emphasize the disadvantages of an in-situ bake-out system being complicated and aperture-consuming.

Use of NEG-coatings has expanded over the recent years due to its advantageous properties and good experience. The latter have shown very long times needed between re-activating the coatings; apparently the coatings almost re-activate themselves when hit by synchrotron radiation.

Despite the complications of an in-situ bake-out system, we have chosen it mainly because of its fast recovery time after any venting of the system. Also, at the relatively modest temperatures (180 C) needed, bake-out elements, based on printed circuits on kapton-foil, and super-insulation like insulation can be rather thin and modestly aperture consuming.

In the main, the vacuum system will consist of:

a. 12 arc vessels in the combined-function magnets
b. 2/3/4 ID chambers
c. 6 simple round tubes between the two combined-function magnets
d. 12 simple round tubes between the arcs and the straight-section vessels
e. a number of special vessels in bumper magnets, septum, diagnostics etc.

Item a will be made in welded stainless steel.

Items b will be extruded aluminium coated with NEG coating (SAES Getters).

It is also planned to coat items b., c. and d. with NEG coating (SAES Getters), which will also be made of stainless steel.

Two cooled copper photon absorbers will be installed in each of the 12 arc-vessels. The absorbers will be electrically isolated allowing them to be used as clearing electrodes too.

2.8.1 Calculations of vacuum performance

2.9 Lifetime considerations (JSN)

2.9.1 Vacuum lifetime

2.9.2 Touschek calculations

2.10 Insertion devices

ASTRID2 is designed with 6 straight sections, and a maximum of four insertion devices possible.

2.10.1 Proposed ID's

Initially, due to financial limitations, only one additional insertion device will be built for ASTRID2 in addition to the existing undulator used in ASTRID since several years. The present undulator will be reused to serve the SGM2/electron-molecular scattering experiment and the SGM3/ARPES monochromator and end-station. A second undulator is being considered, and some parameters also appear in table 10.

The new insertion device will be a high-field multi-pole wiggler to reach as high photon energies as possible.

As ASTRID2 will operate at rather low energy, the influence of the insertion devices on the beam will be significant. This concerns both the tune-change and focusing on the beam but also steering effects from field errors are magnified at low energy and should be minimized.

The multi-pole wiggler, although mounted on a girder with adjustable magnet gap, will be operated at constant magnetic field of 2 T. Although the influence on the beam will be significant, it will be constant, and users will be less affected as compared to varying gap undulators.

Table 10 below shows the main parameters of the existing undulator together with the new multi-pole wiggler.

Two versions of the MPW have been considered: the longest possible (1925 mm) with a rather large gap (18) and a shorter with 700 mm with a gap of 12 mm. We have opted for the shorter MPW, partly for financial reasons, partly because of the influence on the beam, but also because the additional increase in photon flux from the longer device is not considered worthwhile. An additional reason for the shorter MPW is also, that it will be significantly easier to collimate the photon cone and cool away the power.

Table 10 Insertion devices in ASTRID2

Insertion device	**Present ASTRID undulator**	**New undulator**	**Multipole Wiggler**
Period length (λ_u) (mm)	55	65	116 (175)
Number of periods	30	30	6 (11)
Peak magnetic field (T)	0.558	0.80	2.0
Gap (mm)	22-240	18	12 (18)
Inner vacuum gap (mm)	19		8 (14)
K (max)	2.87	4.89	21.7 (32.7)
Max. deflection angle (mrad)			19 (28.8)
Max. deflection angle (°)			
Width after 2 m (mm)			±38 (±5)8
Length (L) (mm)	1650	1950	700 (1925)
Total power radiated (W)	18	54	119 (328)
Transverse roll-off			
Peak field drop at ±5 mm (T)	0.004		
Peak field drop at ±10 mm (T)	0.02		
Peak field drop at ±25 mm (T)	0.135		
Multipole content (at all gaps)			
Dipole (normal and skew)	< 10 Gcm		
Quadrupole (normal and skew)	< 8 G		
Sextupole (normal and skew)	< 8 G/cm^2		
Octupole (normal and skew)	< 2 G/cm^2		
Spectrum quality at minimum gap			
Harmonic #5	92%		
Harmonic # 9	75%		
Harmonic # 15	58%		

2.10.2 Influence of ID's on the beam in ASTRID2

The tune shift of a perfect insertion device is given by

$$\Delta\nu_x = 0, \qquad \Delta\nu_y = \frac{\pi L < \beta_y > K^2}{2\lambda_u^2 \gamma^2},$$

where $<\beta_y>$ is the average of the vertical beta-function in the insertion device, γ is the relativistic gamma factor, and the remaining factors as defined in table 11. The corresponding focusing factors δk_i can be found using the usual small gradient error formula

$$\Delta\nu_i = -\frac{<\beta_i>\delta k_i L}{4\pi}.$$

Using the MatLab Accelerator Toolbox, these focusing factors have then been used to define a 6-by-6 transfer matrix, with a long quadrupole with two independent focusing factors for the horizontal and vertical planes. This matrix is then included in the lattice,

and the influence of the insertion devices have been studied. Table 11 shows the tune changes, Table 12 and 13 the values and the change of the vertical beta function in the middle of the straights. The insertion devices have in this study always been places in SS4 (in the middle of the lattice), but they will of course in reality be placed in various straight sections. Naturally, there is no change in the horizontal beta function. The change in chromaticity is very small, about 2% vertically for the "big" multipole wiggler.

Obviously, the changes in the tune and beta functions are largest for the multi-pole wiggler (MPW). However since the MPW will be operated statically, its influence on the user beams in normal operation is less important. More importantly, we have to learn about and compensate the changes in the lattice functions for the undulators, to allow the users to freely change the undulator gap without affecting the other users too much. Several decisions will have to be made, partly based on experience, on how to minimize the effects of varying gaps in insertion devices. For example, do we want to keep the tunes constant or not? Do we want to compensate the focusing change from an insertion device locally, i.e. only using the nearby quadrupoles?

Table 11 Tune shifts from the various insertion devices

Insertion device	K	L_period [m]	L [m]	N	Tune Shift (V)
"big" MPW	32.7	0.175	1.925	11	0.109
"small" MPW	21.7	0.116	0.700	6	0.042
new undulator	4.89	0.065	1.950	30	0.021
Old undulator, 22 mm gap	2.87	0.055	1.650	30	0.009
Old undulator, 18 mm gap	3.66	0.055	1.650	30	0.014

There will also be a change (reduction) of the emittance of the beam due to the insertion device. This effect will be particularly large for the "big" wiggler, where the radiated power is about a ¼ of the radiated power in the dipoles. This effect has not yet been evaluated in detail yet. Another issue is the influence of the insertion devices on the dynamic aperture considered in the next section. A third issue which needs to be addresses is the influence on the beam lifetime.

Table 12 Vertical beta function values in the center of the 6 straight sections. The insertion device in the simulation is always placed in SS4.

	SS1	SS2	SS3	SS4	SS5	SS6
No insertion device	1.426	1.426	1.426	1.426	1.426	1.426
"big" MPW	0.918	1.595	2.214	0.986	2.214	1.595
"small" MPW	1.111	1.487	1.831	1.338	1.831	1.487
new undulator	1.298	1.439	1.567	1.308	1.567	1.439
Old undulator, 22 mm gap	1.367	1.430	1.489	1.381	1.489	1.430
Old undulator, 18 mm gap	1.332	1.434	1.527	1.355	1.527	1.434

Table 13 The relative change of the vertical beta functions using the data in table 11

	SS1	SS2	SS3	SS4	SS5	SS6
"big" MPW	-36%	12%	55%	-31%	55%	12%
"small" MPW	-22%	4%	28%	-6%	28%	4%
new undulator	-9%	1%	10%	-8%	10%	1%
Old undulator, 22 mm gap	-4%	0%	4%	-3%	4%	0%
Old undulator, 18 mm gap	-7%	1%	7%	-5%	7%	1%

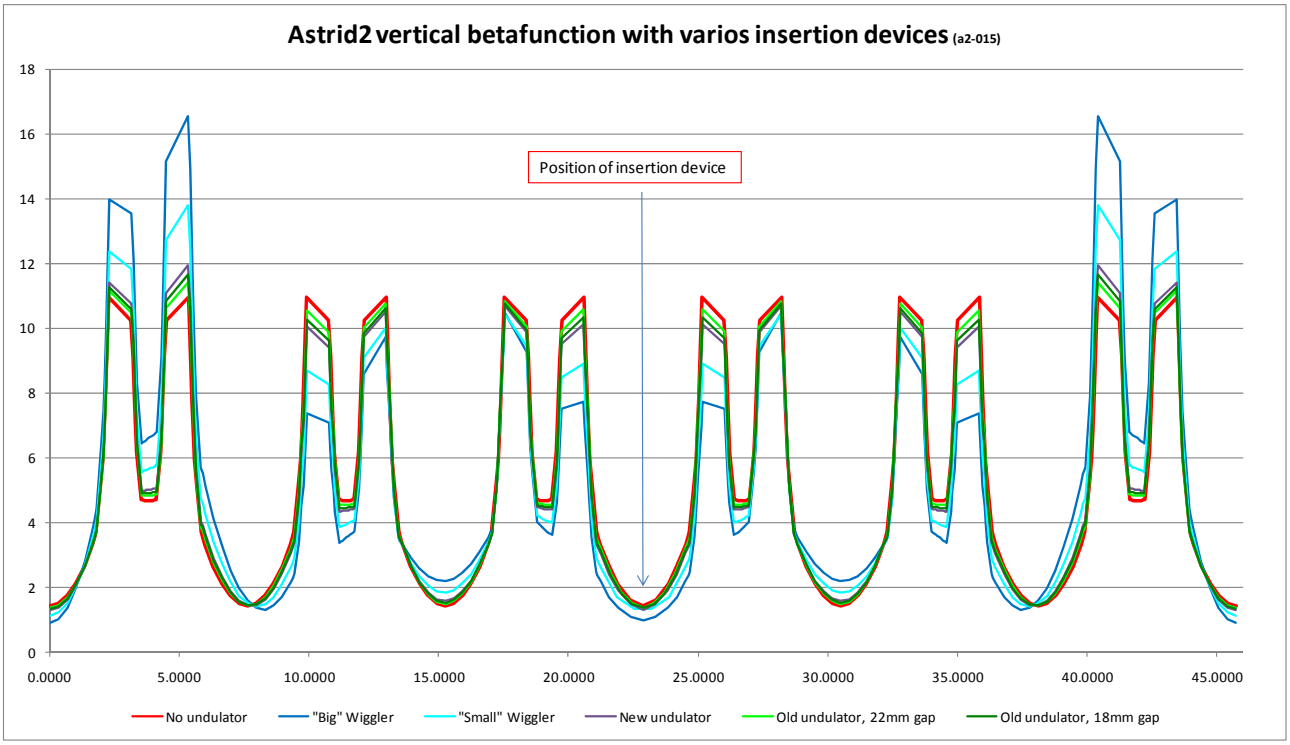

Fig. 18 The vertical beta functions for various insertion devices in ASTRID2.

2.11 Dynamical aperture

For a low-emittance storage ring with strong sextupoles to compensate the large chromaticities studies and optimization of the dynamical aperture is important. For ASTRID2, some effort has been spent to maximize and obtain a sufficiently large dynamical aperture. In particular it was realized, as suggested by L.-J. Lindgren from MAXLAB, that extended sextupolar fields are strongly reducing the dynamical aperture as compared to discrete sextupoles in machines with large radii of curvature, i.e. in small machines. When this principle was implemented, a sufficiently large dynamical aperture could be obtained, not only without insertion devices, but also with insertion devices in all 4 straight sections.

Figure 19 shows the dynamical aperture (in MATLAB) for ASTRID2 without and insertion devices and with insertion devices in all four straight sections, i.e. a MPW, the ASTRID undulator, and two new undulators. Without any insertion devices the dynamical aperture is luxuriously large, and even with 4 insertion devices, the dynamical aperture is

sufficiently large to obtain a large lifetime and allow injection outside the septum situated at 14.5 mm.

The above dynamical aperture plots are made with horizontal and vertical tunes of 5.18, 2.14, respectively. However, the aperture is not very tune-dependent, at least within expected small operational tune-changes of ±0.05.

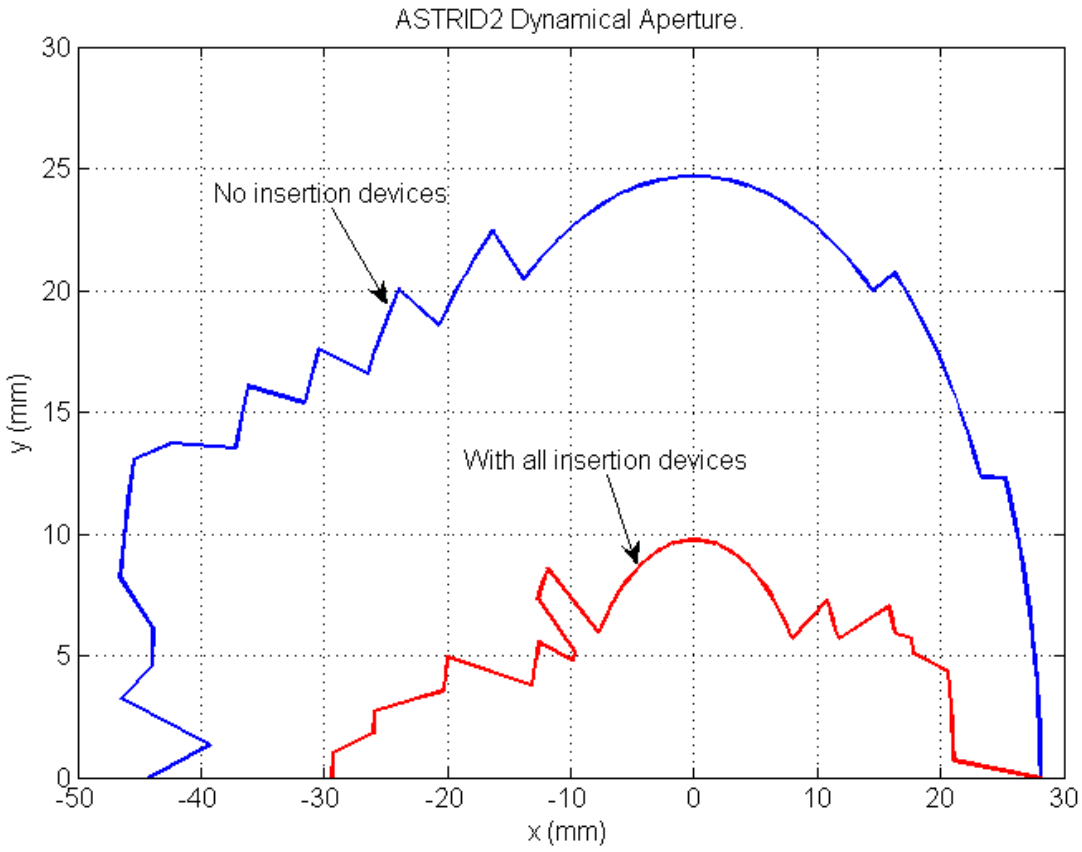

Fig. 19 Dynamical aperture in ASTRID2 with and without insertion devices.

3 MODIFICATIONS TO ASTRID

3.1 Hardware changes to ASTRID

ASTRID is a quadratic machine with four straight sections. The first straight section, SS1, includes primarily a dc septum built for injection, but also used for parasitic extraction of a high energy electron beam. SS2 includes primarily the undulator, whereas SS3 the injection kicker, a tune kicker system and the 105 MHz rf cavity. SS4 contains the electron cooler, to be removed shortly.

For the ASTRID2 project, we have only considering horizontal extraction schemes in ASTRID.

In general, extraction of a beam from one synchrotron to be transferred and injected into another synchrotron is performed with a full-aperture kicker, which kicks the beam across a septum, which deflects the beam out of the synchrotron. Moving the beam close to the septum prior to extraction with a system of bumper magnets may reduce the necessary extraction kicker strength.

3.1.1 Extraction from ASTRID

For the ASTRID2 project, ASTRID will need to be upgraded into a booster for ASTRID2 operating in top-up mode. In the transition period between operation of all synchrotron radiation beamlines on ASTRID and operation of all synchrotron radiation beamlines on ASTRID2, ASTRID will need to alternate on an hourly to weekly basis between operating in synchrotron radiation mode with a long lifetime (>50 hours) and a high current (around 200 mA) and in booster mode, providing a low-intensity beam (~10 mA) with a short repetition cycle (< 30 s). Preferably, swapping between the two modes should be remote controlled with no hardware modifications and a short time delay.

For ASTRID2 operation, a single pulse from the microtron will be injected into ASTRID resulting in an accelerated current up to 10 mA. Optimizing the acceleration and flat-top times, a repetition frequency in excess of 2/min should be possible (!).

It has been demonstrated (JSN, March 2009) that with a high ASTRID injection kicker pulse, a flexibility of several times ±10 kHz of the RF frequency in ASTRID can lead to a sufficiently large current (~10 mA). Hence a direct synchronization between ASTRID and ASTRID2 is planned.

Further tests and optimizations will have to be made in preparation of the ASTRID2 operation. In particular, new and optimized ramping tables will have to be made. This should include an optimized single-shot injection without excitation of the sextupoles for chromaticity correction, high kicker value and possibly zero clearing voltage.

The beam will be extracted from ASTRID during a fraction of a revolution time with a new kicker, which kicks the beam across the present thick DC septum magnet. Although this septum magnet is relatively thick (11 mm), it is preferred to keep this septum to minimize the changes to ASTRID, although clearly a pulsed septum could be made with a much smaller thickness. Hence the fast kicker should have a rise time of less than around 50 ns much less than the revolution time of 133 ns of the circulating beam in ASTRID. No synchronization between the 14 bunches in ASTRID and the kicker is foreseen. There will be available space in ASTRID for this new kicker in SS4, when the electron cooler will be removed. Possibly, but only marginally, there could also be created space in SS3 next to the RF cavity.

The nominal horizontal tune in ASTRID is 2.22. The oscillations of a beam kicked 1 mrad in the beginning of a straight section is shown during the first two turns in fig. 20. For this 1 mrad kick, we observe an amplitude in the straight sections of 5-7 mm after ¼ turn, 10-12 mm after ½ turn and 15 mm after 1 ¼ turn. As it will appear below, a kick of around 20 mm is necessary to jump the septum thickness. In first approximation, this can thus be

provided by a ~3.5 mrad kick for a ¼ turn extraction, ~2 mrad for a ½ turn extraction and ~1 mrad for a 1¼ turn extraction. Hence we are discussing these three extraction schemes below. Remember that in the third case, the beam is kicked twice. As discussed below, limitations in aperture has to be considered by the use of local bumps.

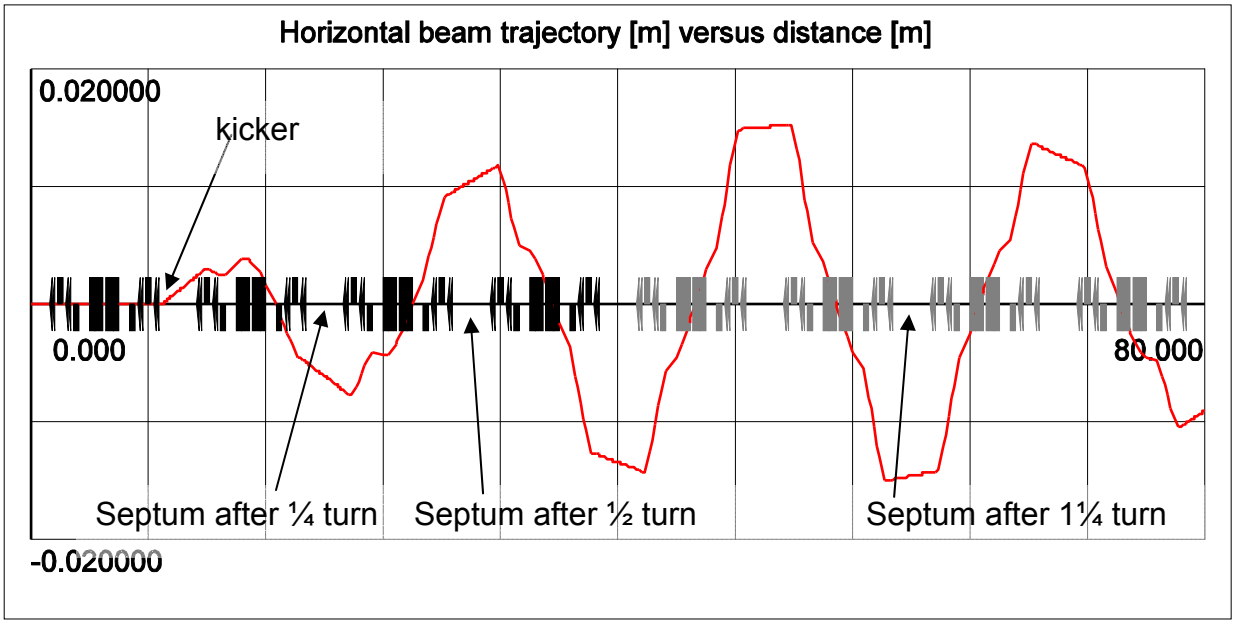

Fig. 20 Two turns in ASTRID after kick of 1 mrad in the beginning of a straight section. Notice the vertical scale of ± 20 mm and the horizontal scale of 80 m, two times the ASTRID circumference.

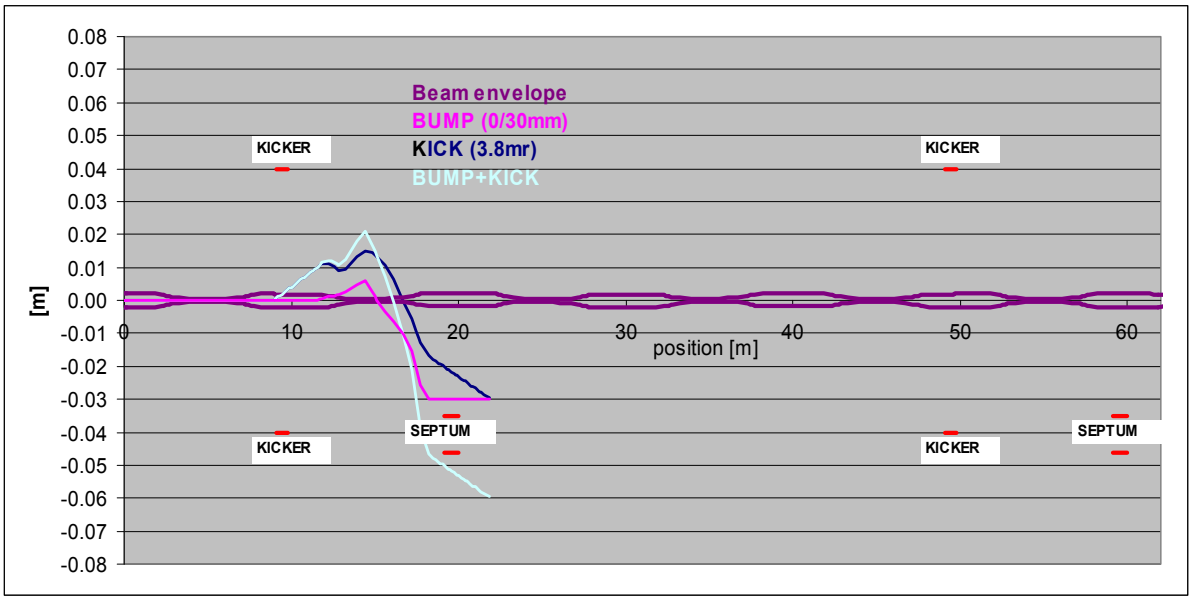

Fig. 21 Extraction after ¼ turn. Notice that the beam is bumped to 30 mm at the septum.

The main parameters of the ASTRID extraction scheme are given in table 14. The horizontal beamsize (rms) in the straight sections is 2.0 or 1.45 mm taking the energy spread into account or not. The total thickness of the ASTRID septum magnet is 11 mm.

The horizontal quantum lifetime is expected to be ~5 s when the beam distance to the septum is 4 rms beam sizes, ~1 s at 3.5 rms and ~0.3 s at 3 rms. In order not to reduce the beam current too much, the bump should only be activated prior to extraction on the high-energy flat-top during as short a time as possible. The corrector magnets of ASTRID can be ramped to their maximum current during a few tenths of a second, and we hence expect the beam to be close to the septum for around 1/10 s. We design the extraction system with a bump of 5 mm inside clearance to the septum before extraction, which should give some contingency in lifetime. For the extracted beam passing close to the septum at the beginning of the extraction channel, we design for a 4 mm outside clearance to the septum. Hence we get a necessary position shift from the kicker of 5 + 11+ 4 mm = 20 mm, stemming from the beam distance from the septum before extraction, the septum thickness and the beam distance from the septum after extraction.

Table 14 **Extraction from ASTRID**

Thickness of septum (coil+vacuum chamber envelope)	11 mm
Distance of inner septum envelope from center of ASTRID	35 mm
Length of septum magnet	852 mm
Distance from end of ASTRID sextupole/corrector to beginning of septum magnet	492 mm
Distance from end of ASTRID sextupole/corrector to beginning extraction kicker magnet	100 (or 400)
Outer acceptance inside septum vacuum chamber	149+11+35 mm
Trajectory bumped at septum	30 mm
Necessary kicked distance at septum	5+11+4=20mm
Corresponding to kick angle for ¼/½/1¼ turn extraction	3.8/2.0/1.7 mrad

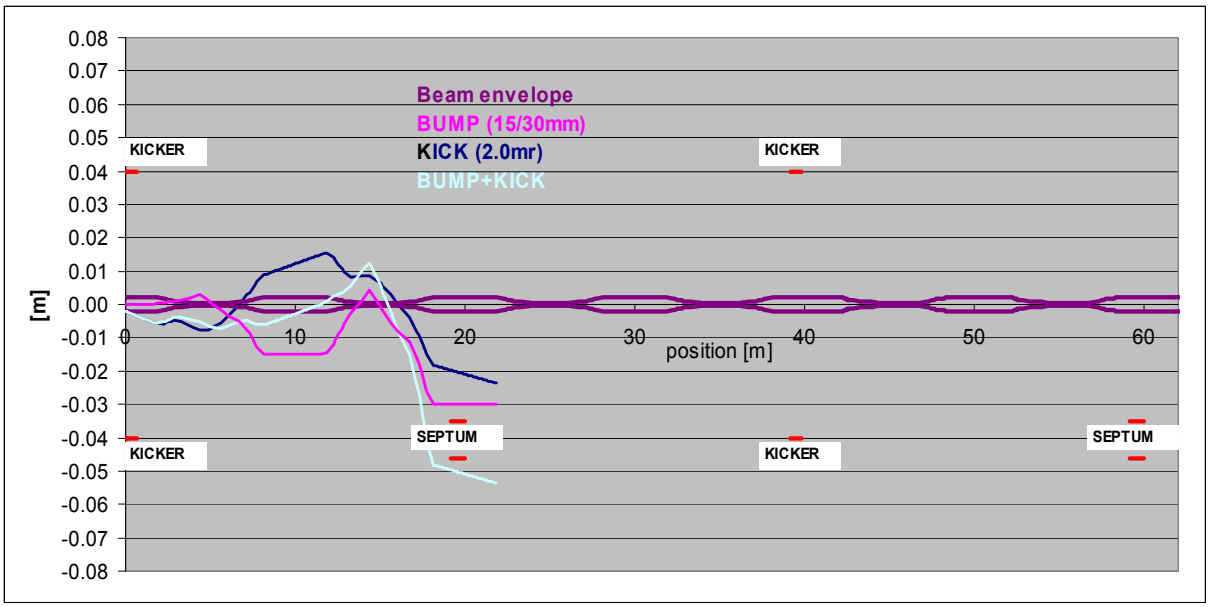

Fig. 22 Extraction after ½ turn. Notice that the beam is bumped 30 mm at the septum.

In fig. 21, 22 and 23 we show the three different extraction schemes corresponding to extraction after ¼ turn, ½ turn and 1 ¼ turn. In addition to showing separately the orbit bump and the kicked beam, we also show the combination of the two leading to extraction. Also the beam envelope is shown around the central axis. In addition the septum coil 35-46 mm from the optical axis, and the horizontal aperture of the kicker of ±40 mm are shown.

The ¼ turn extraction scheme, fig. 22, is conceptually simple, and consist of a fast extraction kicker in SS4 kicking the beam across the septum in SS1. The kicker is placed as early in SS4 as possible. The septum bump is 30 mm and a kick angle of at least 3.8 mrad is needed to kick the beam across the septum.

The ½ turn extraction scheme in fig. 23 is equally simple, and consist of a fast extraction kicker in SS3 kicking the beam across the septum in SS1. A bump of 15 mm in SS4 centers the beam although possibly not necessary. The septum bump is again 30 mm and a kick angle of 2.0 mrad gives a kick of 20 mm at the septum.

The 1 ¼ turn extraction scheme is shown in fig. 24, and consists of a fast extraction kicker in SS4 kicking the beam across the septum in SS1 after 1¼ turns. The beam is hence kicked twice by the extraction kicker.

Such a double-kick extraction scheme was accidentally discovered and used at the booster built for ANKA in Karlsruhe. We see no disadvantage of such a novel extraction scheme, as long as there is sufficient aperture available and furthermore the always needed flexibility in closed-orbit position and angle.

A bump of 20 mm in SS4 is needed to keep the beam within the aperture during its second passage of the kicker. A septum bump of 16 mm reduces the kick angle and still keeps the beam clear of the septum during its first passage, and a kick angle of 1.7 mrad is sufficient to kick the beam 20 mm across the septum.

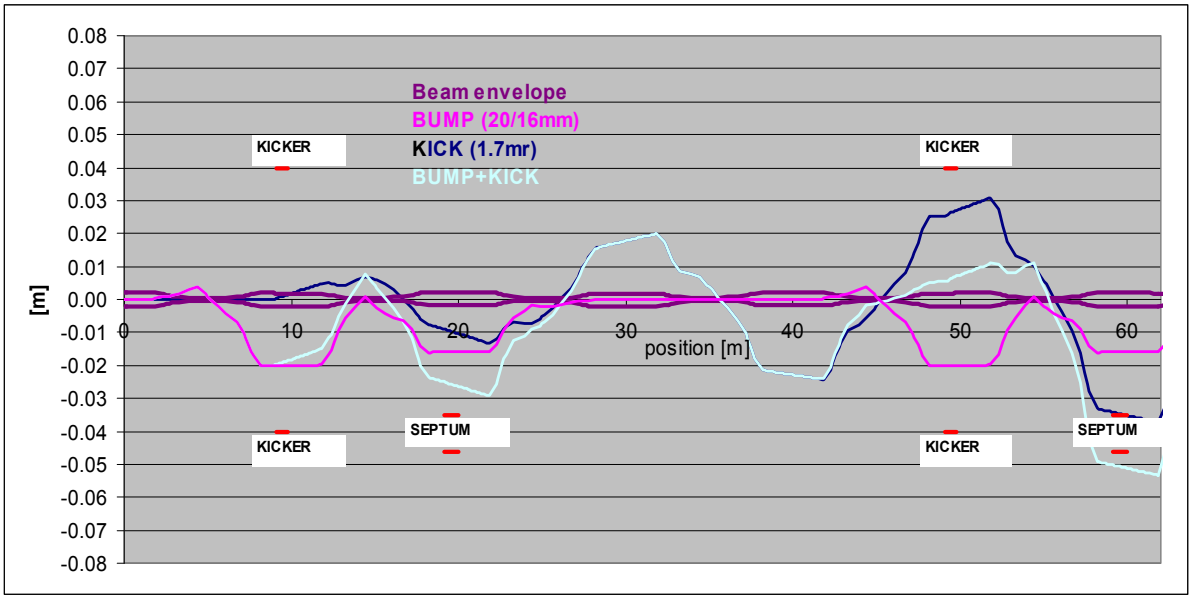

Fig. 23 Extraction after 1¼ turn. Notice that the beam is bumped 20 mm at the kicker and 16 mm at the septum.

We note that for this 1¼ extraction scheme, there is ample distance between the beam and the aperture limiting septum and kicker, as opposed to the ¼ and ½ turn extraction schemes. Hence the actual positioning of the beam is less critical and the beam losses during bumping can be neglected.

In conclusion, we choose the 1¼ turn extraction scheme with its relatively low extraction kicker angle and large distances from apertures. A tracking simulation of the 1¼ turn extraction is shown in fig. 24. The 50 beam particles are generated from the nominal ASTRID emittance and energy spread. The blue tracks are for beam particles during the first revolution after the kicker being fired, whereas the red tracks are for the beam particles after the second kicker passage. We observe the reasonable clearance between the beam particles and the transverse septum position at 35-46 mm.

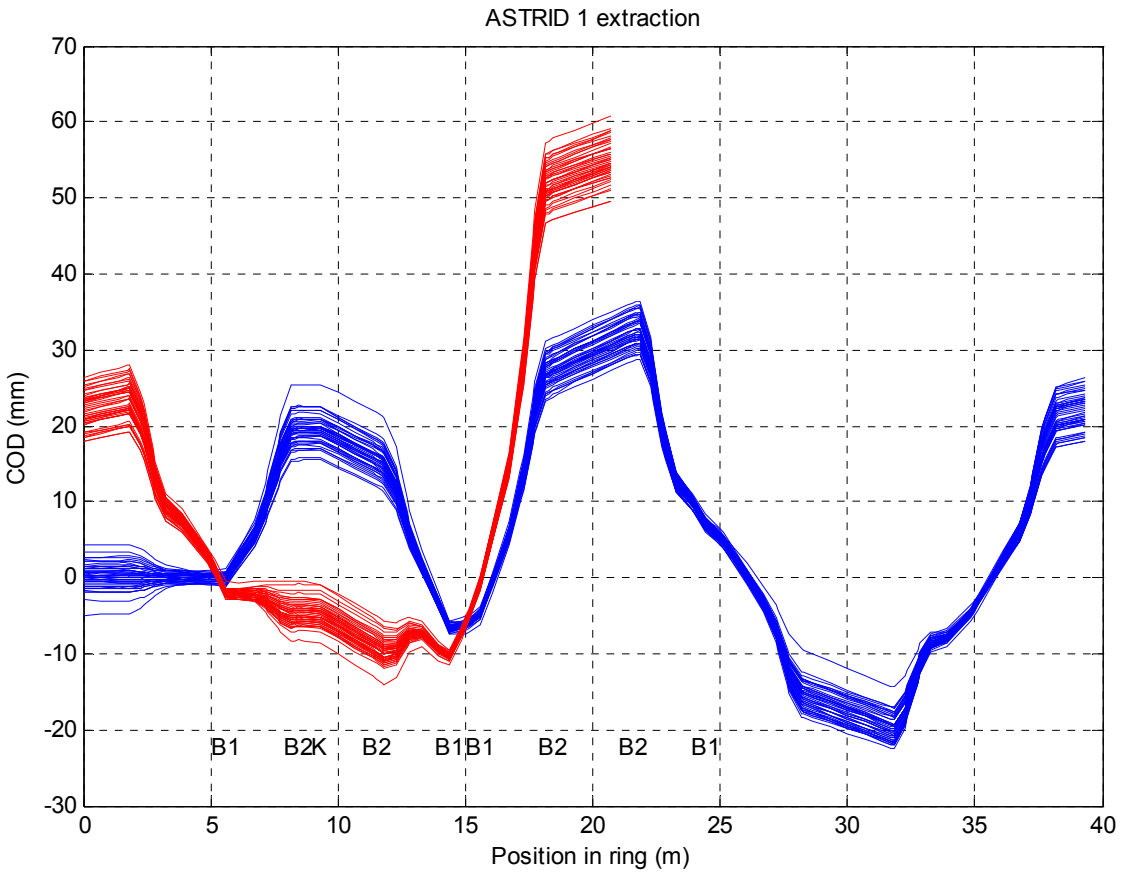

Fig. 24 Tracking of bumped and kicked beam particles for the 1¼ turn extraction scheme.

4 TRANSFER BEAMLINE ASTRID TO ASTRID2

The extracted beam will leave ASTRID through the septum at an angle of 9 degrees with straight section 1 in ASTRID and enter ASTRID2 in straight section 1, which is at an angle of 36 degrees with ASTRID. The beam therefore has to be bent horizontally by an angle of 45º after leaving ASTRID. This is accomplished partly by the ASTRID2 injection septum (15 º), partly by a horizontal bend in the beamline (30º).

In addition, the beamline must pass the ASTRID2 ring. We have chosen to bend the beamline under the ASTRID2 ring mainly for radiation reasons. In the proposed beamline, the injection beamline is lowered 300 mm when passing ASTRID2 making passage through the holes in the girder possible point. This bypass is made by 4 identical vertical dipoles, each bending the beam by 4.3 degrees in a symmetrical way, leading to a vanishing vertical dispersion at the fourth vertically deflecting magnet.

Four quadrupoles are needed for an adequate matching between the two rings. In addition, 4 HV correctors are foreseen, two at each end of the beamline. The total length of the beamline is 21.9 m.

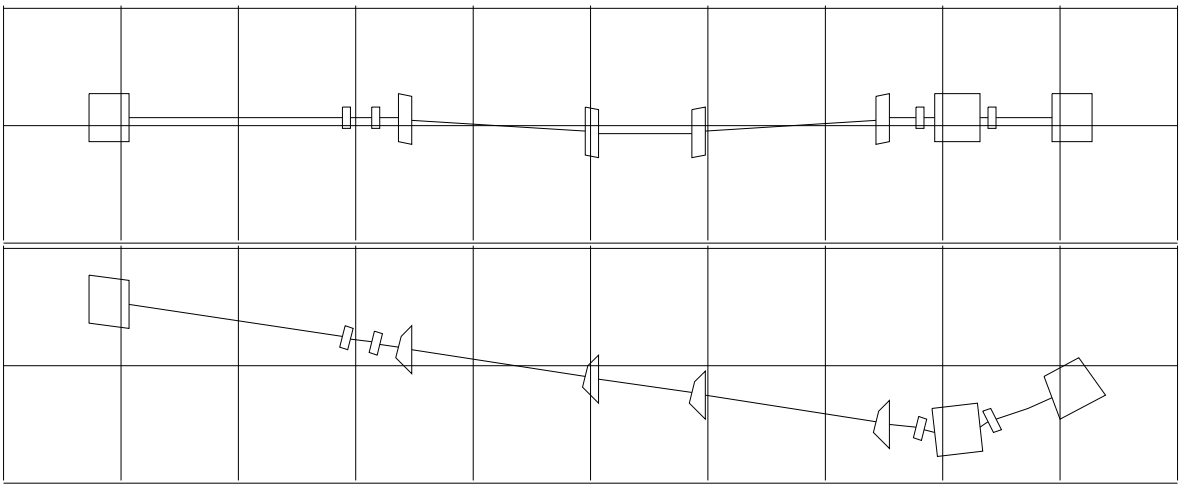

Fig. 25 View of the beamline between ASTRID and ASTRID2 seen from the side and from above. The first element in the beamline is the ASTRID septum magnet, and the last element is the injection septum magnet in ASTRID2.

Because of the very low repetition rate (~0.05Hz) of pulses from ASTRID, the **diagnostics** of the beamline must be sufficient to characterize the beam such that corrections to the optical elements can be calculated and adjusted automatically from shot to shot, i.e. permitting computer controlled alignment. This is achieved by 3 fluorescent screens and 5 Synchrotron-Radiation cameras. The three screens will be mounted after the ASTRID septum, between the two central vertical dipoles and just before the ASTRID2 septum. The five SR cameras will be mounted on the 4 vertical 4.3 deg. dipoles, and the horizontal 30 deg. dipole. The fields in these dipoles will be about 0.48 and 1T resp., which is more than sufficient to generate intense SR for the cameras.

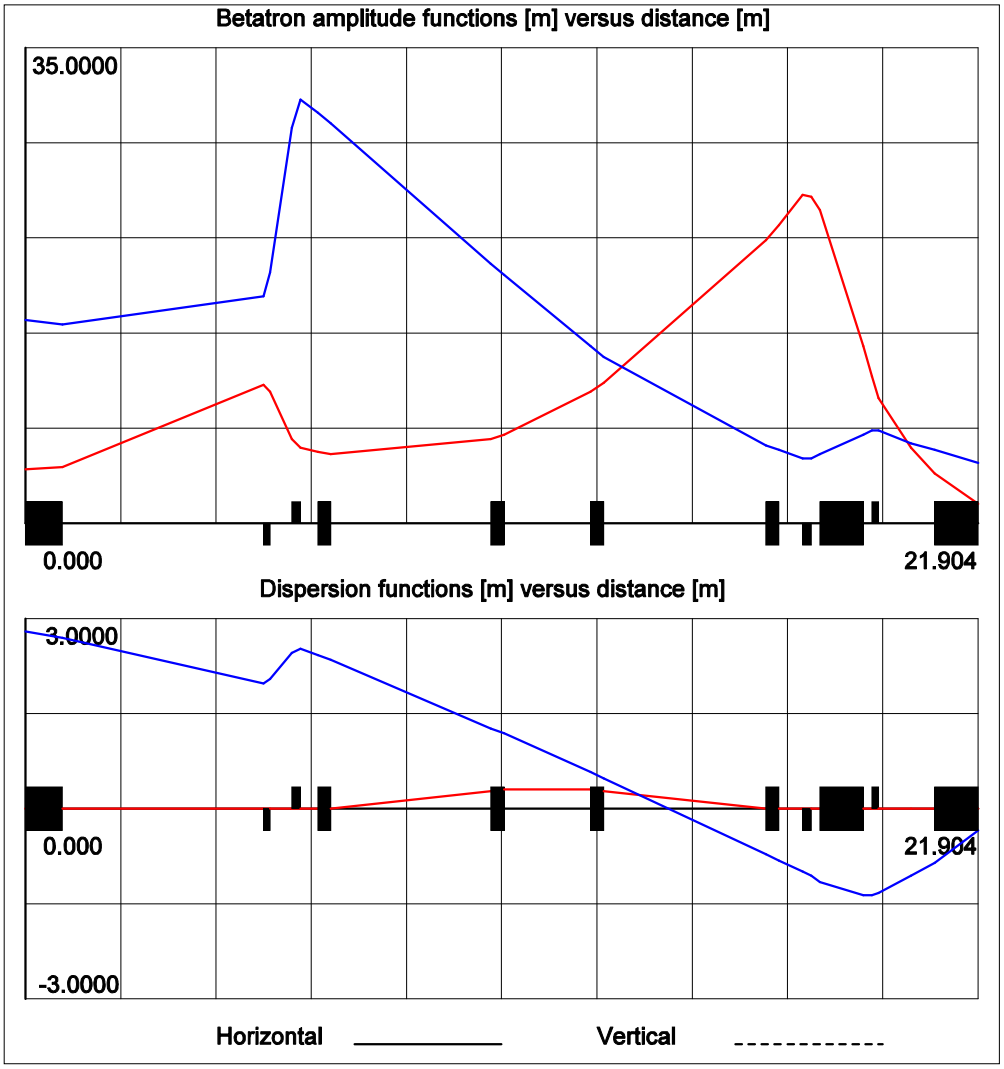

Fig. 26 Twiss parameters of transfer beamline and matching parameters.

It is only necessary to maintain a good **vacuum** near ASTRID and ASTRID2. For this reason, it is planned to mount ion pumps near the two septa and only one in the middle. There will be a sector valve at each end of the beamline, one roughing/venting port and three full-range vacuum gauges.

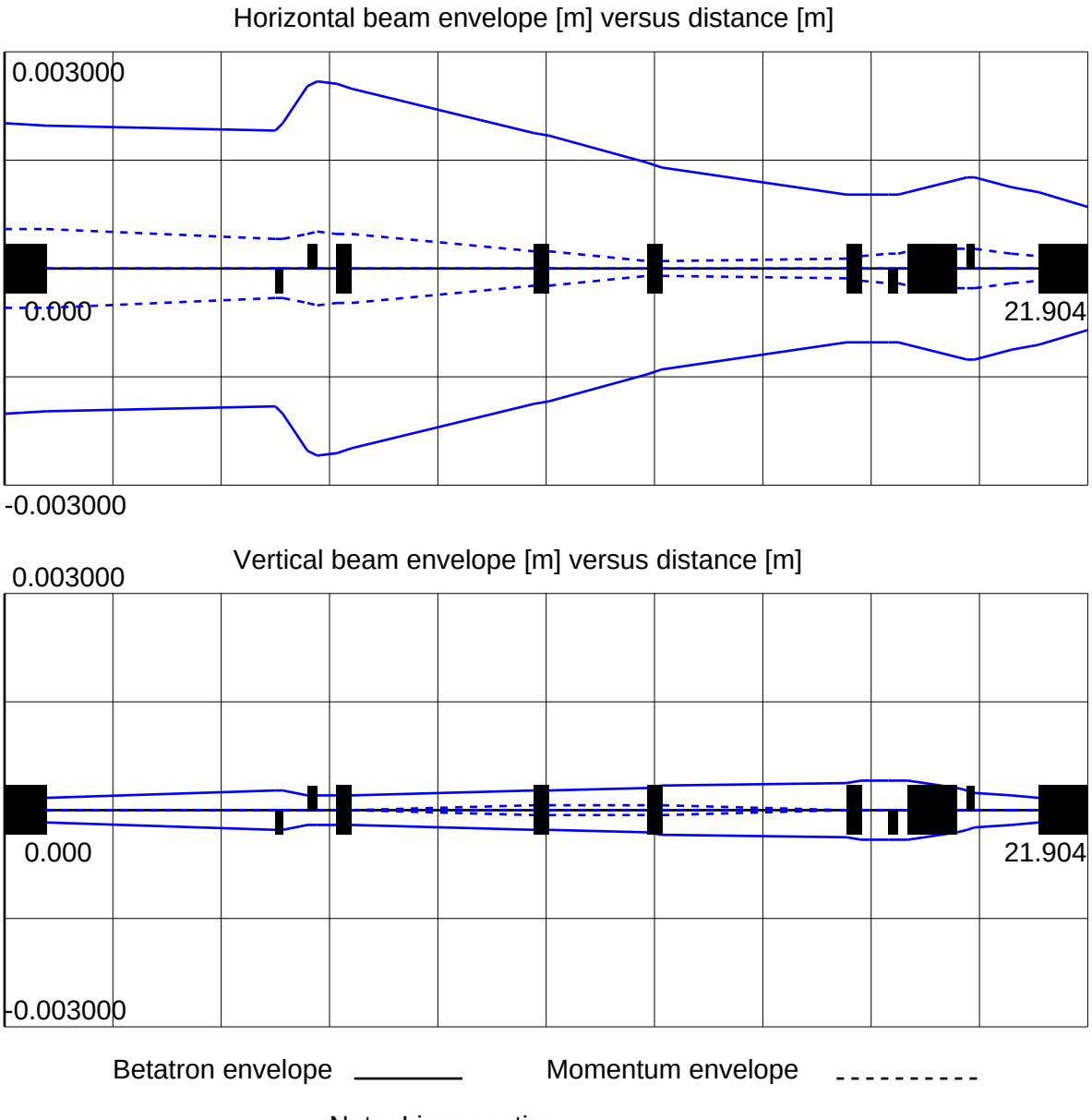

Fig. 27 Beam envelopes (rms) in the transfer beamline between ASTRID and ASTRID2.

5 TOP-UP OPERATION OF ASTRID2

The operation of modern synchrotron-radiation facilities, in particular those of low-emittance, sets strict requirements to stability both in position, angle and current. In addition to maximizing the flux, a circulating current with a long lifetime also helps to keep the beam stable in position and angle by having a stable heat-load on all systems from power supplies to optical components. The ultimate operation consists of the so-called top-up mode, planned for ASTRID2. Here the electrons lost from the beam over a short time interval due to mainly the Touschek effect are replenished. For example a circulating current of 200 mA and a constancy of 2 % in current can be specified, and once the current has dropped below 196 mA, additional shots from ASTRID will be added until the current is again above 200 mA.

For a lifetime of 2 hours and an injected current of 4 mA, a single top-up injection will have to be performed every 144 s to keep the current constant with 196-200 mA.

The consequence of such an operation is that the microtron and ASTRID have to be idle, waiting for the next injection. If ASTRID is waiting at its 0-energy flattop, the idling power consumption will be very small.

Possibly, for stability reasons, the microtron will have to operate with e.g. a repetition frequency of e.g. 1/5 Hz, only injecting into the ASTRID hall when requested, otherwise dumping the beam in the microtron cave.

As for ASTRID, also ASTRID2 will have to be operated outside normal working hours without operator assistance. If top-up mode for some reasons fails, the beam in ASTRID2 will simply decay with its natural lifetime, possibly as short as a few hours at 200 mA.

6 RADIATION SHIELDING AND RADIATION MONITORING (NH)

6.1 Shielding around ASTRID2

A relatively thin (~½m) concrete wall will be built around ASTRID2 matching the ASTRID2 shape using concrete blocks of only a few different shapes. The wall will also have to be adapted to the exiting beamlines and their optical components. In addition, the wall has to be easily demountable for easy access.

The wall thickness can be rather thin partly due to the forward angle (1/sin(30º)=2), partly due to the relatively small number of electrons injected. With the above example, around $4 \cdot 10^9$ electrons at 580 MeV are being lost and injected every 144 s. When aligning the beam in ASTRID, a dose rate of around a factor of 2000 higher is produced.

Two labyrinths are foreseen.

6.2 Shielding around ASTRID, when beamlines have been relocated

As seen in fig.5, a new shielding wall will have to be built around ASTRID in the present ASTRID hall. The wall will in particular separate the SGM3 and SGM2 beamlines from the ASTRID machine itself.

7 ASTRID2 LATTICE

Unit no.	Name	Type	Length [m]	H-bend [rad]	V-bend [rad]	Edge angle-1 [rad]	Edge angle-2 [rad]	k-quad. [m-2]	kk-sext. [m-3]
1		((	0.0000	0.000000	0.000000	0.00000	0.00000	0.000000	0.000000
2	D14837	DRIFT	1.4837	0.000000	0.000000	0.00000	0.00000	0.000000	0.000000
3	BPM	HVPU	0.0000	0.000000	0.000000	0.00000	0.00000	0.000000	0.000000
4	D0100	DRIFT	0.1000	0.000000	0.000000	0.00000	0.00000	0.000000	0.000000
5	QF3	QUADR	0.1800	0.000000	0.000000	0.00000	0.00000	-5.939500	0.000000
6	D0180	DRIFT	0.1800	0.000000	0.000000	0.00000	0.00000	0.000000	0.000000
7	HV	HVCOR	0.0000	0.000000	0.000000	0.00000	0.00000	0.000000	0.000000
8	D0180	DRIFT	0.1800	0.000000	0.000000	0.00000	0.00000	0.000000	0.000000
9	BH	SBEND	0.8500	0.523599	0.000000	0.00000	0.00000	1.678200	0.000000
10	D0190	DRIFT	0.1900	0.000000	0.000000	0.00000	0.00000	0.000000	0.000000
11	SD	SEXTU	0.1500	0.000000	0.000000	0.00000	0.00000	0.000000	81.930000
12	D0120	DRIFT	0.1200	0.000000	0.000000	0.00000	0.00000	0.000000	0.000000
13	QF2	QUADR	0.1800	0.000000	0.000000	0.00000	0.00000	-6.070000	0.000000
14	D0120	DRIFT	0.1200	0.000000	0.000000	0.00000	0.00000	0.000000	0.000000
15	SF	SEXTU	0.0750	0.000000	0.000000	0.00000	0.00000	0.000000	-125.620000
16	BPM	HVPU	0.0000	0.000000	0.000000	0.00000	0.00000	0.000000	0.000000
17	SF	SEXTU	0.0750	0.000000	0.000000	0.00000	0.00000	0.000000	-125.620000
18	D0120	DRIFT	0.1200	0.000000	0.000000	0.00000	0.00000	0.000000	0.000000
19	QF2	QUADR	0.1800	0.000000	0.000000	0.00000	0.00000	-6.070000	0.000000
20	D0120	DRIFT	0.1200	0.000000	0.000000	0.00000	0.00000	0.000000	0.000000
21	SD	SEXTU	0.1500	0.000000	0.000000	0.00000	0.00000	0.000000	81.930000
22	D0190	DRIFT	0.1900	0.000000	0.000000	0.00000	0.00000	0.000000	0.000000
23	BH	SBEND	0.8500	0.523599	0.000000	0.00000	0.00000	1.678200	0.000000
24	D0180	DRIFT	0.1800	0.000000	0.000000	0.00000	0.00000	0.000000	0.000000
25	HV	HVCOR	0.0000	0.000000	0.000000	0.00000	0.00000	0.000000	0.000000
26	D0180	DRIFT	0.1800	0.000000	0.000000	0.00000	0.00000	0.000000	0.000000
27	QF3	QUADR	0.1800	0.000000	0.000000	0.00000	0.00000	-5.939500	0.000000
28	D0100	DRIFT	0.1000	0.000000	0.000000	0.00000	0.00000	0.000000	0.000000
29	BPM	HVPU	0.0000	0.000000	0.000000	0.00000	0.00000	0.000000	0.000000
30	D14837	DRIFT	1.4837	0.000000	0.000000	0.00000	0.00000	0.000000	0.000000
31		)) 6	0.0000	0.000000	0.000000	0.00000	0.00000	0.000000	0.000000
32	End								

8 TIME-LINE OF ASTRID2 PROJECT

SEE NEXT PAGE


APPENDIX 2
19-05-2009
2009
2010
2011
2012
2013
1 2 3 4 5 6 7 8 9 10 11 12
Forskningsinfrastrukturbevilling
Lokaler
149 (ELISA)
153 (Kvantegas)
172 (Birkedal)
141 (SEP1)
166, 167, 169, 170 (Drewsen, Keiding, Stapelfeldt)
145 (ASTRID2) Infrastructure, el, water, shielding
113 (ASTRID) new shielding
ASTRID
IFA MIC. power supplies
ASTRID ion removal
New LLRF
New IFA MPS (injection)
ASTRID extr. Kicker
Production
ASTRID
SR SR SR SR SR SR SR SR SR SR SR SR SR SR SR SR SR SR SR SR Extr
SR A2 SR A2
Transfer Beamline
Magnets
Tender
Production
Support stands
Power supplies
IFA steerer MPS
Vacuum system
Beam diagnostics
Transfer beamline commissioning with beam
ASTRID2
DC magnets
Tender
Production
Pulsed Magnets with PS
Tender
Production
DC Power supplies
Tender
Production
IFA steerer MPS
RF cavity (MAX)
RF transmitter
RF LLRF
Beam diagnostics
Vacuum system
Controls
ASTRID2 MultiPoleWiggler
Design
Tender
Production
ASTRID undulator
ASTRID2 commissioning
SR SR
SR SR
SR SR SR
SR SR
SR SR SR SR SR SR SR SR SR SR SR SR SR
Beamlines
Relocation SX700/SGM1
x-ray microscope?
? ? ? ? ? ?
Relocation SGM2
Relocation SGM3
Abandoning Onduline
Relocation UV1
Relocation CD-1
Milestones
ASTRID2 design report reviewed
X
Magnets and power supplies ordered
X
Detailed layout of ASTRID2 vacuum system
X
Magnets and power supplies delivered in Århus
X
Beam circulating in ASTRID2
X
First user beam on first monochromator on ASTRID2
X
All beamlines in operation on ASTRID2
X
Normal use
End of phase
Removal
Design
Purchase, tender
Production
installation
commissioning with beam